A variational multiscale method to incorporate strain gradients in a phenomenological plasticity model

S.L. Creighton [a], R.A. Regueiro [b], K. Garikipati [a,*], P.A. Klein [b],
E.B. Marin [b], D.J. Bammann [b]

[a] *Department of Mechanical Engineering, University of Michigan, 2278 Brown Building, Ann Arbor, MI 48109-3170, USA*
[b] *Sandia National Laboratories, Livermore, CA 94551, USA*

Abstract

We treat mathematical and computational issues related to the incorporation of strain gradient terms in a phenomenological plasticity model. The strain gradients are associated with incompatibilities due to geometrically necessary dislocations, and are quantified by the Nye dislocation density tensor. When incorporated within a flow rule for the plastic strain rate, this tensor fundamentally alters the mathematical structure of the theory. Several computational complexities also arise as a result. These problems are posed in the setting of a variationally-based multiscale method. It allows the circumvention of some of the mathematical and computational difficulties associated with this model. The phenomenological plasticity model, its enhancement by strain gradients, formulation within a multiscale context and two numerical examples are presented.
© 2004 Elsevier B.V. All rights reserved.

Keywords: Variational multiscale method; Strain gradient; Phenomenological plasticity model

1. Introduction and background

With increasing computational power and more sophisticated diagnostic equipment to investigate material microstructure, high-fidelity material models are being developed under the rubric of multiscale materials modeling [37]. Applications for these models include predictive analysis of mechanical performance of

materials used in solid devices of macroscopic size (centimeter to meter) as well as micro- and nano-systems. Various solid models and modeling approaches can be classified as ''multiscale'', as different models are appropriate for the multiple size scales of a material's response (dislocation-scale to polycrystalline-scale response in metals, for instance). The strain gradient plasticity model presented for computational implementation in this paper is appropriate for phenomenological plasticity, but is motivated by single to multiple-grain response in metals. In particular, this model uses the Nye dislocation density tensor to account for the net density of dislocations of one sign averaged over a number of grains representative of the polycrystalline material [4,22]. These are geometrically-necessary dislocations (GNDs). The study of continuous distributions of dislocations that was popular in the 1950s and 60s [7,25,26,34] has regained interest in the materials modeling community motivated by the current focus on multiscale material modeling [1,3,6,8,15,16,21,23,27,28,32,33,36,39,40]. The model in this paper is similar to the strain gradient models in the above-cited works. The common goal is to represent the effect of GNDs at the continuum scale in polycrystalline metals. Two broad issues arise in the context of computational implementation of these models.

The first issue is whether a robust and efficient methodology can be developed by which these highly complex material models can be incorporated in existing computational codes. Models in advanced mechanics of materials undergo frequent modification and enhancement of constitutive relations to reflect fairly complex physics deduced from experiments. These modifications can often radically alter the mathematical character of the overall system of equations. Reformulations of the computational methods are frequently required, are time-consuming and need revalidation. One approach with potential to overcome some of these difficulties is to view any constitutive relation as a fine scale model that is to be embedded in a coarse scale formulation. In most cases of interest, this coarse scale formulation is merely a weak statement of the balance of linear momentum for a solid. The variational multiscale method that forms the basis of the computational implementation in this work is one possible technique to achieve such a formulation. It involves a scale separation of the displacement into fine and coarse components, which one can associate with fine scale and coarse scale material behavior. In some cases it allows the problem to be posed entirely in terms of coarse scale variables; e.g., displacements on the macroscopic scale, thereby also allowing significant computational efficiency. In this paper, the variational multiscale framework is modified so that the labels of ''fine'' and ''coarse'' scales are no longer entirely appropriate. However, the spirit of the formulation remains the same.

The second issue pertains to the mathematical vagaries that a specific high-fidelity material model introduces to the system of equations describing the mechanics. The strain gradient models of interest explicitly include gradients of various strain measures (the plastic strain or internal elastic strain) in the evolution equation. These gradients result from the incorporation of the density of GNDs in the formulation. The central difficulty is that the plastic strain's evolution is then dictated by a partial differential equation involving space and time, instead of an ordinary differential equation in time. Mathematical (and therefore computational) complications arise as boundary conditions must be specified on plastic strain tensors, the material tangent modulus tensor is nonlocal, and the mathematical well-posedness of the overall model itself is not guaranteed. The multiscale decomposition adopted here, and the manipulation of fine and coarse scale weak forms that is made possible, also allows the circumvention of some of these complications. This variational multiscale method has previously been applied to strain localization problems [19], embedding surface laws in macromechanics [17], and to embedding another fine scale strain gradient plasticity model in the macromechanical formulation [18].

The main body of the paper begins with the phenomenological plasticity model in Section 2. The variational multiscale method for this model is outlined in Section 3. The finite element implementation and numerical results appear in Sections 4 and 5. Conclusions and a discussion are in Section 6.

2. The phenomenological plasticity model

Starting with a strain gradient crystal plasticity model presented by Bammann [6], Regueiro and co-workers [35] formulated a nonlocal phenomenological plasticity model that accounts for the average effect of GNDs over a representative number of grains. With a physically-motivated plastic spin $\overline{W}^{\mathrm{p}}$ and texture effects represented by a structure tensor $\overline{A}$, we can attempt to represent an average physical lattice curvature through $\mathrm{curl}\, F^{\mathrm{e}-1}$, where F^{e} is the elastic deformation gradient, leading to the dislocation density tensor $\overline{\alpha}^{\mathrm{e}}$. In order to focus on the computational implementation, however, it is helpful to simplify the plasticity model. We ignore plastic spin, texture effect on yield, static recovery, and temperature dependence (i.e., an isothermal model), and recognize that without the structure tensor and plastic spin we do not expect a physically meaningful dislocation density tensor. The resulting simplified strain gradient plasticity model is summarized in this section.

2.1. Kinematics

The deformation gradient is multiplicatively decomposed into elastic and plastic parts [7,26,30,29,31,38]. Figs. 1 and 2 show the multiplicative decomposition $F = F^{\mathrm{e}}F^{\mathrm{p}}$ where $\mathscr{S}$ denotes the current configuration, $\mathscr{B}$ the reference configuration, and $\overline{\mathscr{B}}$ the intermediate configuration. We view F^{p} as incompatible plastic deformation associated with dislocations and their motion, and F^{e} as both incompatible lattice deformation causing the deformation to be compatible as well as macroscopic elastic deformation due to external loads. In Fig. 1, $\tilde{F}^{\mathrm{e}}$ is the lattice deformation due to external loading that causes macroscopic stress. This idea is attributed to Bilby [7] and Kröner [26] who were solving the elasticity problem for the internal stress field
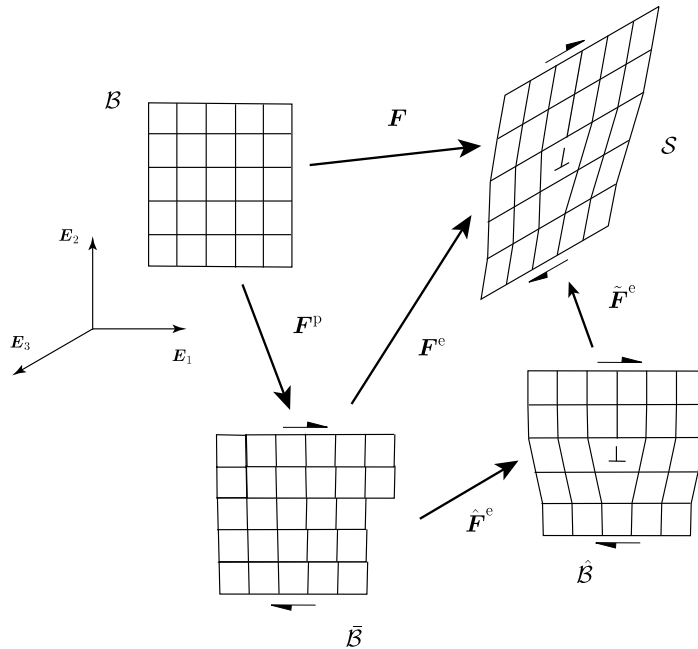
Fig. 1. Single edge dislocation perspective of multiplicative decomposition $F = F^{\mathrm{e}}F^{\mathrm{p}} = \tilde{F}^{\mathrm{e}}\hat{F}^{\mathrm{e}}F^{\mathrm{p}}$. F^{p} and $\hat{F}^{\mathrm{e}}$ are incompatible, and $\tilde{F}^{\mathrm{e}}$ is compatible. F^{p} is the accumulated plastic deformation, or motion of dislocations, and $\hat{F}^{\mathrm{e}}$ is the lattice deformation due to the dislocation defect.
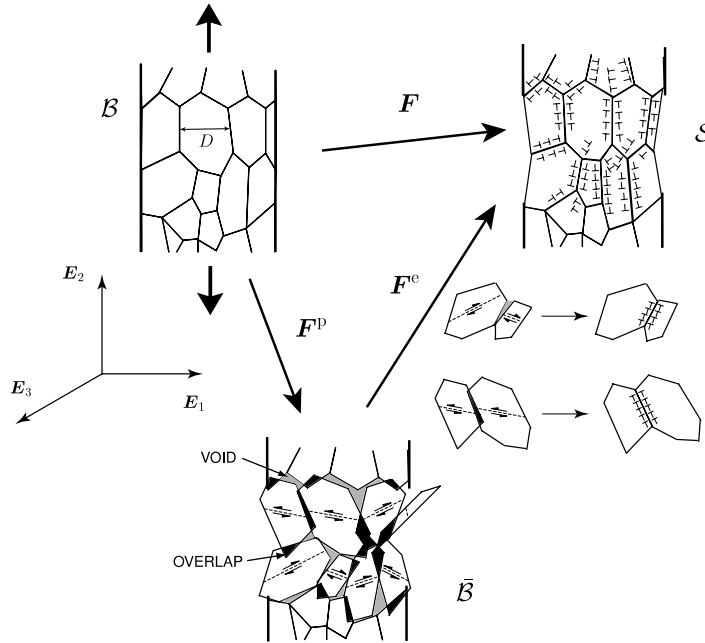
Fig. 2. Polycrystalline perspective of multiplicative decomposition.

due to dislocations. Under small external loads, the dislocation microstructure should remain intact (F^p and $\hat{F}^e$ remain unchanged) while macroscopic stress is generated through $\tilde{F}^e$. In Fig. 2, motivated from Ashby [4] and Naghdi and Srinivasa [32], F^p is incompatible as individual grains shear along their various slip systems and attempt to misorient with respect to each other. The incompatible part of F^e makes the deformation compatible by introducing GNDs at or near grain or sub-grain boundaries, while the compatible part of F^e is lattice stretching and rotation due to external loads.

The velocity gradient l in the current configuration is written

$$l = \dot{F}F^{-1} = \dot{F}^e F^{e-1} + F^e \dot{F}^p F^{p-1} F^{e-1} = l^e + l^p, \tag{1}$$

where the plastic velocity gradient in the intermediate configuration is $\overline{L}^p = \dot{F}^p F^{p-1}$. The velocity gradient may be additively decomposed as the rate of deformation tensor d and spin w in the current configuration as $l = d + w$, $d := \mathrm{sym}(l)$ and $w := \mathrm{skew}(l)$. The plastic deformation rate d^p may be written in terms of its intermediate configuration counterpart as

$$l^p = d^p = \mathrm{sym}(F^e \overline{L}^p F^{e-1}) = F^{e-T} \overline{D}^p F^{e-1}; \quad w^p = 0, \tag{2}$$

where $\overline{D}^p := \mathrm{sym}(\overline{C}^e \overline{L}^p)$ is the plastic deformation rate in $\overline{\mathscr{B}}$, $\overline{C}^e = F^{eT} F^e$ is the elastic right Cauchy–Green tensor, and plastic spin is ignored ($w^p = 0$). The elastic strain in the intermediate configuration is $\overline{E}^e := \frac{1}{2}(\overline{C}^e - \overline{1})$.

The local compatibility conditions read [9,26,36]

$$\begin{aligned} \mathrm{Curl}F &= \mathrm{Curl}(F^e F^p) = 0, \\ \mathrm{curl}\,F^{-1} &= \mathrm{curl}\,(F^{p-1} F^{e-1}) = 0. \end{aligned} \tag{3}$$

These local compatibility conditions state that any microstructural misorientation or curvature (at the grain or sub-grain scale) attempting to create voids or to overlap material is restricted for continuum deforma-

tion. In the context of finite deformation, [9,36] these compatibility conditions were used to derive the lattice curvature deformation tensors in the intermediate configuration. This gives the Nye dislocation density tensor [34]; cf. Regueiro and co-workers [35] for notation:

$$\overline{\boldsymbol{\alpha}}^{\mathrm{e}} - \overline{\boldsymbol{\alpha}}^{\mathrm{p}} = \mathbf{0},$$
$$\overline{\boldsymbol{\alpha}}^{\mathrm{e}} = -J^{\mathrm{e}} \boldsymbol{F}^{\mathrm{e}-1} \cdot (\operatorname{curl} \boldsymbol{F}^{\mathrm{e}-1})^{\mathrm{T}}, \quad J^{\mathrm{e}} = \det \boldsymbol{F}^{\mathrm{e}},$$
$$\overline{\boldsymbol{\alpha}}^{\mathrm{p}} = -\frac{1}{J^{\mathrm{p}}} \boldsymbol{F}^{\mathrm{p}} \cdot (\operatorname{Curl} \boldsymbol{F}^{\mathrm{p}})^{\mathrm{T}}, \quad J^{\mathrm{p}} = \det \boldsymbol{F}^{\mathrm{p}} = 1. \tag{4}$$

The lattice curvature measured by the Nye dislocation density tensor, $\overline{\boldsymbol{\alpha}}^{\mathrm{e}}$, representing the average density of GNDs will be used to calculate an unsymmetric internal stress tensor associated with hardening by GNDs. In order to calculate stress, a deformation measure that is dimensionally consistent with a strain measure is needed. Hence, a length scale l is introduced as

$$\overline{\boldsymbol{\alpha}}_l^{\mathrm{e}} := l \overline{\boldsymbol{\alpha}}^{\mathrm{e}}. \tag{5}$$

Refer to Bammann [6] for further discussion of the length scale l and unsymmetric dislocation stress $\overline{\boldsymbol{\zeta}}$ requiring angular momentum balance.

2.2. Thermodynamics

Here, the thermodynamics are summarized, following the thermodynamic formulations by Coleman and co-workers [11] and [10]. Assume that the mass-specific Helmholtz free energy function in the intermediate configuration depends on compatible lattice deformation due to external mechanical forces, $\overline{\boldsymbol{E}}^{\mathrm{e}}$, lattice deformation due to the presence of statistically stored dislocations, $\overline{\epsilon}_{ss}$, lattice curvature due to the presence of GNDs at grain or sub-grain boundaries and around second phase particles, $\overline{\boldsymbol{\alpha}}_l^{\mathrm{e}}$, and absolute temperature, $\theta : \psi = \hat{\psi}(\overline{\boldsymbol{E}}^{\mathrm{e}}, \overline{\epsilon}_{ss}, \overline{\boldsymbol{\alpha}}_l^{\mathrm{e}}, \theta)$.

Standard thermodynamic arguments [10,11] are used to motivate the following constitutive relations:

$$\overline{\boldsymbol{S}} = \overline{\rho} \frac{\partial \psi}{\partial \overline{\boldsymbol{E}}^{\mathrm{e}}}, \quad \overline{\eta} = -\frac{\partial \psi}{\partial \theta}, \tag{6}$$

where $\overline{\rho}$ is mass density in $\overline{\mathscr{B}}$, $\overline{\boldsymbol{S}}$ is the second Piola–Kirchhoff stress in $\overline{\mathscr{B}}$ resulting from compatible stretching of the lattice through $\boldsymbol{F}^{\mathrm{e}}$, and $\overline{\eta}$ is the entropy. Defining the stress-like internal state variables conjugate to $\dot{\overline{\epsilon}}_{ss}$ and $\dot{\overline{\boldsymbol{\alpha}}}_l^{\mathrm{e}}$ respectively as

$$\overline{\kappa} := \overline{\rho} \frac{\partial \psi}{\partial \overline{\epsilon}_{ss}}, \quad \overline{\boldsymbol{\zeta}} := \overline{\rho} \frac{\partial \psi}{\partial \overline{\boldsymbol{\alpha}}_l^{\mathrm{e}}}, \tag{7}$$

where $\overline{\kappa}$ is the scalar internal stress field in the lattice due to statistically stored dislocations and $\overline{\boldsymbol{\zeta}}$ is the internal unsymmetric stress field due to GNDs, the dissipation inequality reads

$$\overline{\boldsymbol{S}} : \overline{\boldsymbol{D}}^{\mathrm{p}} - \overline{\kappa} \dot{\overline{\epsilon}}_{ss} - \overline{\boldsymbol{\zeta}} : \dot{\overline{\boldsymbol{\alpha}}}_l^{\mathrm{e}} - \frac{1}{\theta} \overline{\boldsymbol{Q}} \cdot \overline{\nabla} \theta \geqslant 0, \tag{8}$$

where $\overline{\boldsymbol{Q}}$ is the heat flux into $\overline{\mathscr{B}}$. The mechanical quantities in Eq. (8) are interpreted as the plastic deformation work rate per unit mass contributing to dissipation due to dislocation motion $(\overline{\boldsymbol{S}} : \overline{\boldsymbol{D}}^{\mathrm{p}})$, minus the stored work due to the generation and annihilation of statistically stored dislocations $(\overline{\kappa} \dot{\overline{\epsilon}}_{ss})$ and GNDs $(\overline{\boldsymbol{\zeta}} : \dot{\overline{\boldsymbol{\alpha}}}_l^{\mathrm{e}})$; i.e., plastic deformation is dissipative but also leads to stored lattice elastic energy due to the presence of dislocations.

2.3. Constitutive model

The free energy ψ is written in quadratic form as

$$\overline{\rho}\hat{\psi} := \tfrac{1}{2}\overline{\boldsymbol{E}}^{\mathrm{e}} : \mathbb{C} : \overline{\boldsymbol{E}}^{\mathrm{e}} + \tfrac{1}{2}c_{\kappa}\mu\overline{\epsilon}_{ss}^{2} + \tfrac{1}{2}c_{\zeta}\mu\overline{\boldsymbol{\alpha}}_{l}^{\mathrm{e}} : \overline{\boldsymbol{\alpha}}_{l}^{\mathrm{e}} + \overline{g}(\theta), \tag{9}$$

where $\mathbb{C} = \lambda\overline{\boldsymbol{1}} \otimes \overline{\boldsymbol{1}} + 2\mu\overline{\boldsymbol{I}}$ is the fourth order modulus tensor approximated by linear isotropic elasticity, λ and μ are Lamé parameters where μ is the shear modulus, c_{κ} and c_{ζ} are material constants, and $\overline{g}(\theta)$ is the thermal component of the free energy.

The constitutive equations in the intermediate configuration result as

$$\overline{\boldsymbol{S}} = \mathbb{C} : \overline{\boldsymbol{E}}^{\mathrm{e}}; \quad \overline{\eta} = -\frac{\partial\psi}{\partial\theta},$$
$$\overline{\kappa} = c_{\kappa}\mu\overline{\epsilon}_{ss}; \quad \overline{\zeta} = c_{\zeta}\mu\overline{\boldsymbol{\alpha}}_{l}^{\mathrm{e}}. \tag{10}$$

The macroscopic stress $\overline{\boldsymbol{S}}$ and internal dislocation stress $\overline{\zeta}$ will be calculated directly from $\boldsymbol{F}^{\mathrm{e}}$. The internal scalar elastic strain $\overline{\epsilon}_{ss}$ and plastic part of the deformation gradient $\boldsymbol{F}^{\mathrm{p}}$ are determined by integration of evolution equations, which will in turn provide $\boldsymbol{F}^{\mathrm{e}}$ through $\boldsymbol{F}^{\mathrm{e}} = \boldsymbol{F} \cdot \boldsymbol{F}^{\mathrm{p}-1}$, assuming $\boldsymbol{F}^{\mathrm{p}}$ is invertible.

The evolution equation for lattice deformation due to the presence of statistically stored dislocations (ignoring static recovery) is

$$\dot{\overline{\epsilon}}_{ss} = [H - R_{\mathrm{d}}\overline{\epsilon}_{ss}]\dot{\overline{\epsilon}}^{\mathrm{p,eff}}, \tag{11}$$

where $\dot{\overline{\epsilon}}^{\mathrm{p,eff}}$ is the effective plastic strain rate, H is the dimensionless hardening parameter, and R_{d} is the dimensionless dynamic recovery parameter. Eq. (11) is integrated to obtain $\overline{\epsilon}_{ss}$ which in turn provides the internal stress variable $\overline{\kappa} = c_{\kappa}\mu\overline{\epsilon}_{ss}$. We may also write the evolution of the internal stress $\overline{\kappa}$ in rate form as

$$\dot{\overline{\kappa}} = [c_{\kappa}\mu H - R_{\mathrm{d}}\overline{\kappa}]\dot{\overline{\epsilon}}^{\mathrm{p,eff}}. \tag{12}$$

The plastic deformation rate $\overline{\boldsymbol{D}}^{\mathrm{p}}$ is defined separately by its magnitude and direction as

$$\overline{\boldsymbol{D}}^{\mathrm{p}} := \|\overline{\boldsymbol{D}}^{\mathrm{p}}\|\overline{\boldsymbol{N}}^{\mathrm{p}}, \quad \|\overline{\boldsymbol{D}}^{\mathrm{p}}\| = \sqrt{\frac{3}{2}}\dot{\overline{\epsilon}}^{\mathrm{p,eff}}, \quad \overline{\boldsymbol{N}}^{\mathrm{p}} := \mathrm{sym}\left(\frac{\partial\overline{\Phi}}{\partial\overline{\boldsymbol{\Xi}}}\right) \Big/ \left\|\mathrm{sym}\left(\frac{\partial\overline{\Phi}}{\partial\overline{\boldsymbol{\Xi}}}\right)\right\|, \tag{13}$$

where evolution of plastic flow $\dot{\overline{\epsilon}}^{\mathrm{p,eff}}$ is written in unified creep plasticity form as [5]:

$$\dot{\overline{\epsilon}}^{\mathrm{p,eff}} = f\sinh\left[\frac{\langle\overline{\Xi}^{\mathrm{eff}} - (\overline{\kappa} + Y)t\rangle}{V}\right] = \overline{\Phi}, \quad \overline{\Xi}^{\mathrm{eff}} = \sqrt{\frac{3}{2}}\|\overline{\boldsymbol{\Xi}}\|, \quad \overline{\boldsymbol{\Xi}} = \mathrm{dev}\overline{\boldsymbol{S}} - \mathrm{dev}\overline{\zeta}, \tag{14}$$

$$\mathrm{dev}\overline{\boldsymbol{S}} = \overline{\boldsymbol{S}} - \tfrac{1}{3}(\overline{\boldsymbol{C}}^{\mathrm{e}} : \overline{\boldsymbol{S}})\overline{\boldsymbol{C}}^{\mathrm{e}-1}; \quad \mathrm{dev}\overline{\zeta} = \overline{\zeta} - \tfrac{1}{3}(\overline{\boldsymbol{C}}^{\mathrm{e}} : \overline{\zeta})\overline{\boldsymbol{C}}^{\mathrm{e}-1}, \tag{15}$$

where $\langle\bullet\rangle$ is the Macaulay bracket. Since there is no flow surface for this model, the plastic potential function $\overline{\Phi}$ is used to define the direction of plastic flow $\overline{\boldsymbol{N}}^{\mathrm{p}}$. The parameter f in Eq. (14)$_1$ determines the strain-rate at which the model undergoes a transition from rate-independent to rate-dependent behavior [5], V determines the rate-sensitivity of the yield stress, and Y is the quasi-static yield stress. Note that $\overline{\boldsymbol{\Xi}}$ is unsymmetric since $\overline{\zeta}$ is unsymmetric. As a result, $\overline{\boldsymbol{N}}^{\mathrm{p}}$ is defined as the symmetric part of $\partial\overline{\Phi}/\partial\overline{\boldsymbol{\Xi}}$ since $\overline{\boldsymbol{D}}^{\mathrm{p}}$ is symmetric. The kinetic equation for $\dot{\overline{\epsilon}}^{\mathrm{p,eff}}$ describing the velocity of statistically stored dislocations as a function of flow stress is motivated by previous work in the literature [5,20,24]. The direction of associated plastic flow is

$$\overline{N}^{\mathrm{p}} = \mathrm{sym}\left(\frac{\partial \overline{\Xi}^{\mathrm{eff}}}{\partial \overline{\Xi}}\right) \bigg/ \left\|\mathrm{sym}\left(\frac{\partial \overline{\Xi}^{\mathrm{eff}}}{\partial \overline{\Xi}}\right)\right\|; \quad \frac{\partial \overline{\Xi}^{\mathrm{eff}}}{\partial \overline{\Xi}} = \sqrt{\frac{3}{2}}\frac{\overline{\Xi}}{\|\overline{\Xi}\|}. \tag{16}$$

With constitutive equations in place, the evolution for F^{p} is

$$\dot{F}^{\mathrm{p}} = \overline{C}^{\mathrm{e}-1} \cdot \left[\overline{D}^{\mathrm{p}}(F^{\mathrm{p}}, \mathrm{Curl}F^{\mathrm{p}})\right] \cdot F^{\mathrm{p}}, \tag{17}$$

which can be written as an evolution equation for F^{e} as

$$\frac{\partial(F^{\mathrm{e}-1})}{\partial t} = \overline{C}^{\mathrm{e}-1} \cdot \left[\overline{D}^{\mathrm{p}}(F^{\mathrm{e}}, \mathrm{curl}\, F^{\mathrm{e}-1})\right] \cdot F^{\mathrm{e}-1} - F^{\mathrm{e}-1} \cdot l \tag{18}$$

from which F^{p} and F^{e} are calculated. This is a nonlinear, first order partial differential equation for $F^{\mathrm{e}-1}$.

3. A variational multiscale formulation

To place ideas in context we first review the displacement incompatibility that underlies the mathematical theory of plasticity. Section 2 has demonstrated the incompatibility of the intermediate configuration, which is obtained via the mapping F^{p}. This means that F^{p} is not related to the gradient of a displacement. In order to illustrate the ideas we will use the following, rather simple, representation of the incompatibility for single slip: Denoting the one-dimensional Heaviside function by $H_\Gamma(X)$, where

$$H_\Gamma(X) := \begin{cases} 0 : X_1 < \Gamma, \\ 1 : X_1 \geqslant \Gamma, \end{cases} \tag{19}$$

it follows that for single slip $F^{\mathrm{p}} = 1 + vX_2 E_1 \otimes E_2 H_\Gamma(X)$ is globally incompatible, but locally compatible in regions $\Omega^- := \{X \in \Omega | X_1 < \Gamma\}$ and $\Omega^+ := \{X \in \Omega | X_1 \geqslant \Gamma\}$ (see Fig. 3). We can define a displacement field at a point $X = \{X_1, X_2, X_3\}$ as

$$u^\alpha(X) = vX_2 E_1 H_\Gamma(X), \tag{20}$$

where $u^\alpha = 0$ at $X_1 = 0$. This also allows us to introduce $F^\alpha := 1 + \partial u^\alpha / \partial X$, which can be expanded as,

$$F^\alpha = 1 + vE_1 \otimes E_2 H_\Gamma(X) + vX_2 E_1 \otimes E_1 \delta_\Gamma(X), \tag{21}$$
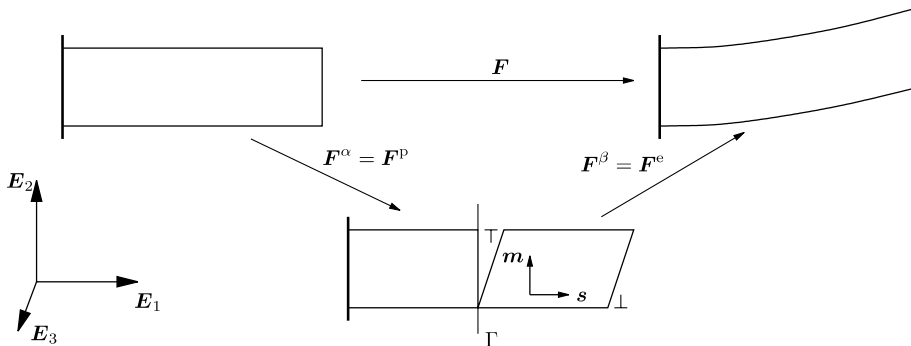
Fig. 3. The incompatible intermediate configuration arising due to single slip. The compatibility of the final configuration is restored by the elastic stretch and rotation from the intermediate configuration. The final configuration in the figure is obtained if the slip corresponding to F^{p} increases along the E_1 direction.

where $\delta_\Gamma(X)$ is the one-dimensional Dirac delta function, and arises as the gradient field of $H_\Gamma(X)$. Of interest here is the fact that $\text{Reg}[F^\alpha] = F^p$, where $\text{Reg}(\bullet)$ denotes the regular part of a field. For our purpose, a regular field is one in which no term is a Dirac delta function. Thus, u^α is related to F^p through Eqs. (20), (21) and $\text{Reg}[F^\alpha] = F^p$. Where F^p is locally compatible it is the gradient of a displacement field, u^α. Formally, we define u^α as

$$\int_\mathscr{C} \frac{\partial u^\alpha}{\partial X} \, \mathrm{d}X = \int_\mathscr{C} (F^p - \mathbf{1}) \, \mathrm{d}X \tag{22}$$

over a contour $\mathscr{C}$ along which F^p is compatible. Incompatibilities in the intermediate configuration arise at points (also curves or surfaces) such as Γ where F^p is discontinuous. At such incompatibilities, we let u^α develop a discontinuity given by $[\![u^\alpha]\!] = u^\alpha|_{\Gamma^+} - u^\alpha|_{\Gamma^-}$.

Since it can be related to slip at the atomic scale, u^α may be thought of as a fine scale field. However, plastic deformation typically dominates the elastic deformation in problems of interest, and this nomenclature can prove confusing. Therefore we will refer to u^α as the α-field in what follows. It is emphasized that u^α is not a physical displacement. In particular, it is not a ''plastic displacement''. However, it allows us to address issues arising with strain gradient plasticity formulations. In particular, boundary conditions can be applied on u^α.

Having thus obtained u^α we define the coarse scale field $u^\beta := u - u^\alpha$ and the corresponding deformation gradient.

$$F^\beta := \mathbf{1} + \frac{\partial u^\beta}{\partial X} \{\text{Reg}[F^\alpha]\}^{-1}. \tag{23}$$

As the elastic deformation is typically smaller than plastic deformation, we will avoid the use of the term ''coarse'' scale to refer to u^β, preferring instead the term β-field. Since the total displacement, u, is compatible, u^β must have a discontinuity that cancels $[\![u^\alpha]\!]_\Gamma$ at each incompatibility. It therefore follows that F^β is also singular. However, $\text{Reg}[F^\beta] = F^e$ as is verified by the following calculation.

Fig. 4 depicts single crystal plasticity, with the further restriction to single slip. The placement of a material point in the reference ($\mathscr{B}$), intermediate ($\overline{\mathscr{B}}$) and spatial configurations ($\mathscr{S}$) is X, $\overline{X}$ and x respectively. Given the deformation gradient F, slip γ, slip plane normal m, and slip direction s, we have $\dot{F}^p F^{p-1} = \gamma s \otimes m$ and $F^e = F F^{p-1}$. Now, decomposing the displacement mathematically as $u = u^\beta + u^\alpha$, we have $\varphi(X) =$
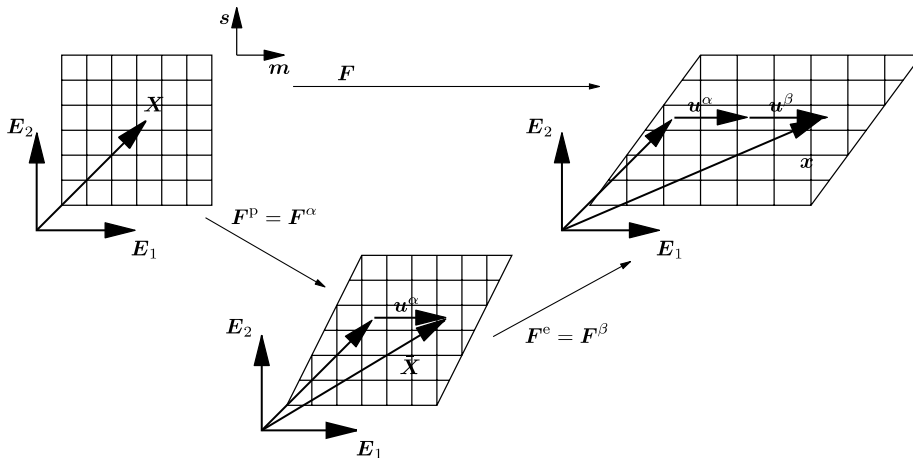
Fig. 4. α-scale (u^α) and β-scale (u^β) displacements motivated by single slip.

$X + u^\beta + u^\alpha$. Recalling that u^α is the displacement that maps the material point to its intermediate placement in $\overline{\mathscr{B}}$, gives $F^\alpha = 1 + \partial u^\alpha / \partial X$ where $\text{Reg}[F^\alpha] = F^p$ as shown previously. Furthermore,

$$
\begin{aligned}
F &= 1 + \frac{\partial u^\beta}{\partial X} + \frac{\partial u^\alpha}{\partial X} \\
&= 1 + \text{Reg}\left[\frac{\partial u^\beta}{\partial X}\right] + \text{Reg}\left[\frac{\partial u^\alpha}{\partial X}\right] \\
&= \underbrace{\left(1 + \text{Reg}\left[\frac{\partial u^\beta}{\partial X}\right]\{\text{Reg}[F^\alpha]\}^{-1}\right)}_{\text{Reg}[F^\beta]=F^e} \underbrace{\left(1 + \text{Reg}\left[\frac{\partial u^\alpha}{\partial X}\right]\right)}_{\text{Reg}[F^\alpha]=F^p}.
\end{aligned}
\tag{24}
$$

Since $\text{Reg}[F^\alpha] = F^p$, we have $\text{Reg}[F^\beta] = F^e$ as indicated.

3.1. Extension to phenomenological continuum plasticity

The incompatibilities are of the order of an Angstrom (roughly the magnitude of the Burgers vector). Since they are restricted to dislocations and grain boundaries, the resulting strain gradients are small when measured at continuum scales (0.1 μm and above). At the continuum scale, therefore, the influence of incompatibilities in plastic deformation is much diminished. At this scale it is therefore a reasonable approximation to treat plastic deformation as compatible, and write F^p as the gradient of a compatible displacement field:

$$
\frac{\partial u^\alpha}{\partial X} := F^p - 1, \quad \frac{\partial u^\beta}{\partial X} F^{\alpha-1} := F F^{p-1} - 1.
\tag{25}
$$

Thus, with the effect of plastic incompatibility being small, the approximations we will use are $F^\alpha = F^p$, $F^\beta = F^e$.

3.1.1. A fundamental difficulty with incompatibilities
From Eqs. (2) and (25) we have

$$
l^p = F^\beta \nabla \dot{u}^\alpha.
\tag{26}
$$

Likewise, Eq. (25) also allows us to write, after some manipulation:

$$
F^e = F^\beta = (1 - \nabla u^\beta)^{-1}.
\tag{27}
$$

A fundamental difficulty now arises when we attempt to use (25) in the phenomenological continuum plasticity model of Section 2. The influence of GNDs is felt in the backstress, $\overline{\zeta}$, that depends on $(\text{curl}\, F^{e-1})^T$ through $\overline{\alpha}_l^e$ [Eqs. (4), (5) and (10)]. On account of Eq. (27), $\overline{\alpha}_l^e = 0$, and the effect of incompatibilities is lost. This is a natural outcome of the assumption that, at the continuum scale, the incompatibilities have a negligible influence.

3.1.2. Weak representation of an incompatible strain field
In order to re-introduce incompatibilities to the multiscale kinematics, we define a strain field ε^β weakly related to ∇u^β:

$$
\int_{\mathscr{S}} \Gamma^\beta : \left(\varepsilon^\beta - \nabla u^\beta\right) \mathrm{d}v = 0.
\tag{28}
$$

Here, Γ^β is a variation on ε^β. The strain field, ε^β, belongs to a space of functions, $\mathscr{E}^\beta$, with the property $\text{curl}\, \varepsilon^\beta \neq 0$ for any function in this space. From Eqs. (4), (27) and (28) the Nye dislocation density tensor

can now be calculated as $\overline{\boldsymbol{\alpha}}_l^{\mathrm{e}} = J^{\mathrm{e}} \boldsymbol{F}^{\mathrm{e}-1}(-\operatorname{curl} \boldsymbol{\varepsilon}^\beta)^{\mathrm{T}} = J^\beta \boldsymbol{F}^{\beta^{-1}}(-\operatorname{curl} \boldsymbol{\varepsilon}^\beta)^{\mathrm{T}}$. The space $\mathscr{E}^\beta$ must be carefully chosen to incorporate incompatibilities in order that $\overline{\boldsymbol{\alpha}}_l^{\mathrm{e}}$ retains the characteristics desired for a given problem. Of course, for numerical solutions, this entails some understanding of the nature of the incompatibility field. In spirit, this is similar to the incorporation of discontinuous interpolation functions in strain localization problems [2]. The linearized form of (28) is

$$\int_{\mathscr{S}} \boldsymbol{\Gamma}^\beta : (\boldsymbol{\varepsilon}^\beta - \nabla \boldsymbol{u}^\beta) \, \mathrm{d}v + \int_{\mathscr{S}} \boldsymbol{\Gamma}^\beta : \delta \boldsymbol{\varepsilon}^\beta \, \mathrm{d}v = 0. \tag{29}$$

3.2. Weak formulation of the phenomenological plasticity model incorporating incompatibilities

This mathematical structure can now be applied to the phenomenological plasticity model of Section 2. Recall that Eq. (17) is a partial differential equation for $\boldsymbol{F}^{\mathrm{p}}$, and Eq. (18) a partial differential equation for $\boldsymbol{F}^{\mathrm{e}}$. Integrating the plastic flow rule therefore requires the solution of either of these partial differential equations. However, this complication can be eased by adopting the multiscale decomposition as we now proceed to demonstrate.

On using Eqs. (2) and (26) in $\overline{\boldsymbol{L}}^{\mathrm{p}} = \dot{\boldsymbol{F}}^{\mathrm{p}} \boldsymbol{F}^{\mathrm{p}-1} = \overline{\boldsymbol{C}}^{\mathrm{e}-1} \overline{\boldsymbol{D}}^{\mathrm{p}}$, we have the following evolution law for $\nabla \dot{\boldsymbol{u}}^\alpha$:

$$\boldsymbol{F}^\beta \nabla \dot{\boldsymbol{u}}^\alpha = [(\boldsymbol{1} - \nabla \boldsymbol{u}^\beta)^{\mathrm{T}} \overline{\boldsymbol{D}}^{\mathrm{p}} (\boldsymbol{1} - \nabla \boldsymbol{u}^\beta)], \tag{30}$$

where $\overline{\boldsymbol{D}}^{\mathrm{p}}$ is governed by the constitutive relations in (13)–(16). With the multiscale decomposition, Eq. (27) and $\overline{\boldsymbol{\alpha}}_l^{\mathrm{e}} = J^\beta \boldsymbol{F}^{\beta^{-1}}(-\operatorname{curl} \boldsymbol{\varepsilon}^\beta)^{\mathrm{T}}$, the right-hand side depends entirely upon gradients of $\boldsymbol{u}^\beta$ and $\boldsymbol{\varepsilon}^\beta$. The relations are complicated, but retain the advantage of being direct functional evaluations. If $\boldsymbol{u}^\beta$ is known, $\boldsymbol{\varepsilon}^\beta$ follows from (28), and $\boldsymbol{u}^\alpha$, is entirely specified if Eq. (30) can be solved.

There then remains the problem of solving the partial differential equation (30) for $\boldsymbol{u}^\alpha$. Since it is of first order in $\boldsymbol{u}^\alpha$, boundary conditions must be specified on some *proper subset* of the boundary of the domain over which this equation is to be solved. We will call this the α-scale subdomain, denoted $\mathscr{B}^\alpha$, and satisfying $\mathscr{B}^\alpha \subset \mathscr{B}$. Since $\boldsymbol{u}^\alpha$ is motivated by slip in crystal plasticity, this displacement field can be specified on the boundary of the plastic domain. This necessitates tracking the evolution of $\mathscr{B}^\alpha$ as plastic flow progresses. In other boundary value problems where slip is constrained on a subset of the displacement boundary $\partial \mathscr{B}_u$, the boundary condition can be specified as $\boldsymbol{u}^\alpha = \boldsymbol{0}$ on $\partial \mathscr{B}_{u^\alpha}$, where $\partial \mathscr{B}_{u^\alpha} \subseteq \partial \mathscr{B}_u$. Having thus specified the boundary conditions on $\boldsymbol{u}^\alpha$, Eq. (30) can be solved via the following α-scale weak form:

$$\int_{\mathscr{S}} \nabla \boldsymbol{w}^\alpha : [\boldsymbol{F}^\beta \nabla \dot{\boldsymbol{u}}^\alpha] \, \mathrm{d}v = \int_{\mathscr{S}} \nabla \boldsymbol{w}^\alpha : [(\boldsymbol{1} - \nabla \boldsymbol{u}^\beta)^{\mathrm{T}} \overline{\boldsymbol{D}}^{\mathrm{p}} (\boldsymbol{1} - \nabla \boldsymbol{u}^\beta)] \, \mathrm{d}v, \tag{31}$$

where $\boldsymbol{w}^\alpha$ is the α-scale weighting function satisfying $\boldsymbol{w}^\alpha = \boldsymbol{0}$ on $\partial \mathscr{B}_{u^\alpha} \subseteq \partial \mathscr{B}_u$. The right hand-side remains a functional evaluation of $\boldsymbol{u}^\beta$ and $\boldsymbol{\varepsilon}^\beta$. In a time-discrete solution, $\dot{\boldsymbol{u}}^\alpha$ is replaced by $\Delta \boldsymbol{u}^\alpha / \Delta t$, where $\Delta \boldsymbol{u}^\alpha = (\boldsymbol{u}^\alpha)_{n+1}^{i+1} - (\boldsymbol{u}^\alpha)_n$ (i being the iteration number and n the time step) and $\Delta t = t_{n+1} - t_n$:

$$\int_{\mathscr{S}} \nabla \boldsymbol{w}^\alpha : \left[\boldsymbol{F}_{n+\vartheta}^\beta (\nabla \Delta \boldsymbol{u}^\alpha) \right] \mathrm{d}v = \Delta t \int_{\mathscr{S}} \nabla \boldsymbol{w}^\alpha : [(\boldsymbol{1} - \nabla \boldsymbol{u}^\beta)^{\mathrm{T}} \overline{\boldsymbol{D}}^{\mathrm{p}} (\boldsymbol{1} - \nabla \boldsymbol{u}^\beta)]_{n+\vartheta} \, \mathrm{d}v, \tag{32}$$

and ϑ refers to a generalized trapezoidal integration $(\bullet)_{n+\vartheta} = \vartheta (\bullet)_{n+1} + (1 - \vartheta) (\bullet)_n$.

3.3. β-scale equations and linearization

The β-scale equation is the following weak form of balance of linear momentum:

$$\int_{\mathscr{B}} \nabla \boldsymbol{w}^\beta : \boldsymbol{\tau} \, \mathrm{d}V = \int_{\mathscr{B}} \boldsymbol{w}^\beta \cdot \boldsymbol{f} \, \mathrm{d}V + \int_{\partial \mathscr{B}_t} \boldsymbol{w}^\beta \cdot \boldsymbol{t} \, \mathrm{d}\Gamma, \tag{33}$$

where $\boldsymbol{\tau}$ is the Kirchhoff stress, $\boldsymbol{f}$ the body force in $\mathscr{B}$, and $\boldsymbol{t}$ the traction. Eqs. (32) and (33) are nonlinearly dependent upon the strains in the finite strain setting, and, as is the practice, they must be expanded up to terms of first order to set up an iterative solution. For strain gradient plasticity models in which a partial differential equation must be solved for $\boldsymbol{F}^{\mathrm{p}}$ or $\boldsymbol{F}^{\mathrm{e}}$, the resulting elastoplastic tangent tensor is nonlocal. A direct numerical implementation becomes unrealistically cumbersome and computationally intensive.

However, this difficulty can be circumvented in the present case due to the multiscale decomposition. For the first order expansion of (33), two approaches are possible: We are interested in calculating the Gateaux variation $\mathrm{d}(\nabla^{\epsilon}w^{\beta}:\boldsymbol{\tau}^{\epsilon})/\mathrm{d}\epsilon|_{\epsilon=0}$, which is the algorithmic version of $\partial(\nabla w^{\beta}:\boldsymbol{\tau})/\partial t$. In the time-exact setting we can use:

$$\begin{aligned}\frac{\partial}{\partial t}(\nabla w^{\beta}:\boldsymbol{\tau}) &= \nabla w^{\beta}:(-\boldsymbol{\tau}\boldsymbol{l}^{\mathrm{T}}+\mathscr{L}_{v}\boldsymbol{\tau}+\boldsymbol{l}\boldsymbol{\tau}+\boldsymbol{\tau}\boldsymbol{l}^{\mathrm{T}}), \\ &= \nabla w^{\beta}:(\mathbb{C}^{\mathrm{ep}}:\boldsymbol{d}+\boldsymbol{l}\boldsymbol{\tau})\end{aligned} \tag{34}$$

or,

$$\begin{aligned}\frac{\partial}{\partial t}(\nabla w^{\beta}:\boldsymbol{\tau}) &= \nabla w^{\beta}:(-\boldsymbol{\tau}\boldsymbol{l}^{\mathrm{T}}+\mathscr{L}_{v}^{\mathrm{e}}\boldsymbol{\tau}+\boldsymbol{l}^{\mathrm{e}}\boldsymbol{\tau}+\boldsymbol{\tau}\boldsymbol{l}^{\mathrm{eT}}), \\ &= \nabla w^{\beta}:(-\boldsymbol{\tau}\boldsymbol{l}^{\mathrm{pT}}+\mathbb{C}:\boldsymbol{d}^{\mathrm{e}}+\boldsymbol{l}^{\mathrm{e}}\boldsymbol{\tau}),\end{aligned} \tag{35}$$

where the first equation comes about by relating the material time derivative of $\boldsymbol{\tau}$ to its Lie derivative, $\mathscr{L}_{v}\boldsymbol{\tau}$, and the second by relating it to the *elastic* Lie derivative, $\mathscr{L}_{v}^{\mathrm{e}}\boldsymbol{\tau}$. The elastic tangent is $\mathbb{C}$, and $\mathbb{C}^{\mathrm{ep}}$ is the elastoplastic tangent. Traditionally, the use of the elastic Lie derivative has been avoided because it results in some elastic and plastic velocity gradient terms, and specifying boundary conditions on the corresponding displacements is problematic. However, with the multiscale decomposition, the use of the algorithmic counterpart of the elastic Lie derivative actually becomes feasible. First let us note that the algorithmic versions of Eqs. (34) and (35) are, respectively,

$$\begin{aligned}\frac{\mathrm{d}}{\mathrm{d}\epsilon}(\nabla^{\epsilon}w^{\beta}:\boldsymbol{\tau}^{\epsilon})|_{\epsilon=0} &= \nabla w^{\beta}:(\mathscr{L}_{\delta u}\boldsymbol{\tau}+(\nabla\delta u^{\beta}+\nabla\delta u^{\alpha})\boldsymbol{\tau}), \\ &= \nabla w^{\beta}:(\mathbb{C}^{\mathrm{ep}}:(\nabla\delta u^{\beta}+\nabla\delta u^{\alpha})+(\nabla\delta u^{\beta}+\nabla\delta u^{\alpha})\boldsymbol{\tau}),\end{aligned} \tag{36}$$

and,

$$\begin{aligned}\frac{\mathrm{d}}{\mathrm{d}\epsilon}(\nabla^{\epsilon}w^{\beta}:\boldsymbol{\tau}^{\epsilon})|_{\epsilon=0} &= \nabla w^{\beta}:(\nabla\delta u\boldsymbol{\tau}+\mathscr{L}_{\delta u^{\beta}}\boldsymbol{\tau}-2\mathrm{sym}(\boldsymbol{F}^{\beta}\nabla\delta u^{\alpha}\boldsymbol{\tau})), \\ &= \nabla w^{\beta}:((\nabla\delta u^{\beta}+\nabla\delta u^{\alpha})\boldsymbol{\tau}+\mathbb{C}^{\mathrm{e}}:\nabla\delta u^{\beta}-2\mathrm{sym}(\boldsymbol{F}^{\beta}\nabla\delta u^{\alpha}\boldsymbol{\tau})).\end{aligned} \tag{37}$$

Now the second set of equations can be rendered in a form depending on u^{β} and ε^{β} if δu^{α} can be solved for in terms of u^{β} and ε^{β} from Eq. (32). Such a linearization of the stress through the elastic strain (here, through the Lie derivative along δu^{β}) is computationally feasible if we can specify boundary conditions on u^{β}. These are obtained as:

$$u^{\beta}+u^{\alpha}=u \Rightarrow u^{\beta}+\mathscr{G}_{\mathscr{B}}^{\alpha}[u^{\beta},\nabla u^{\beta},-\mathrm{curl}\,\varepsilon^{\beta}]=g \quad \text{on } \partial\mathscr{B}_{u}, \tag{38}$$

where $u^{\alpha}=\mathscr{G}_{\mathscr{B}}^{\alpha}[u^{\beta},\boldsymbol{F}^{\beta},\mathrm{curl}\,\varepsilon^{\beta}]$ is a formal representation of the solution to Eq. (32). Observe that the weak form of the β-scale problem is now:

$$\begin{aligned}\int_{\mathscr{B}}[\nabla w^{\beta}:\mathbb{C}^{\mathrm{e}}:\nabla\delta u^{\beta}+\boldsymbol{1}:\nabla\delta u^{\beta}\boldsymbol{\tau}\nabla w^{\beta\mathrm{T}}-2\nabla w^{\beta}:\mathrm{sym}(\boldsymbol{F}^{\beta}\nabla\delta u^{\alpha}\boldsymbol{\tau})+\boldsymbol{1}:\nabla\delta u^{\alpha}\boldsymbol{\tau}\nabla w^{\beta\mathrm{T}}]\,\mathrm{d}V \\ =\int_{\mathscr{B}}w^{\beta}\cdot\boldsymbol{f}\;\mathrm{d}V+\int_{\partial\mathscr{B}_{t}}w^{\beta}\cdot\boldsymbol{t}\,\mathrm{d}\Gamma-\int_{\mathscr{B}}\nabla w^{\beta}:\boldsymbol{\tau}\,\mathrm{d}V+\frac{\mathrm{d}}{\mathrm{d}\epsilon}\int_{\partial\mathscr{B}_{u}\setminus\partial\mathscr{B}_{u^{\alpha}}}w^{\beta}\cdot\boldsymbol{\tau}^{\epsilon}\boldsymbol{F}^{-T^{\epsilon}}\boldsymbol{N}\,\mathrm{d}\Gamma\bigg|_{\epsilon=0}.\end{aligned} \tag{39}$$

The last term on the right hand-side appears since, for w^β, we now have:

$$w^\beta = \mathbf{0} \quad \text{on } \partial\mathscr{B}_{u^\alpha}, \qquad w^\beta \neq \mathbf{0} \quad \text{on } \partial\mathscr{B} \setminus \partial\mathscr{B}_{u^\alpha}. \tag{40}$$

This term must also be linearized using:

$$\frac{\mathrm{d}}{\mathrm{d}\epsilon} \int_{\partial\mathscr{B}_u \setminus \partial\mathscr{B}_{u^\alpha}} w^\beta \cdot \tau^\epsilon F^{-\mathrm{T}\epsilon} N \, \mathrm{d}\Gamma \bigg|_{\epsilon=0} = \int_{\partial\mathscr{B}_u \setminus \partial\mathscr{B}_{u^\alpha}} w^\beta \cdot \left(\mathscr{L}_{\delta u^\beta} \tau + 2\mathrm{sym}(\nabla \delta u^\beta \tau) - 2\mathrm{sym}(F^\beta \nabla u^\beta \nabla \delta u^\alpha \tau) \right) F^{-\mathrm{T}} N \, \mathrm{d}\Gamma$$
$$- \int_{\partial\mathscr{B}_u \setminus \partial\mathscr{B}_{u^\alpha}} w^\beta \cdot \tau (\nabla \delta u^\beta + \nabla \delta u^\alpha)^{\mathrm{T}} F^{-\mathrm{T}} N \, \mathrm{d}\Gamma. \tag{41}$$

Similarly, the α-scale weak form is linearized:

$$\int_{\mathscr{S}} \nabla w^\alpha : [F^\beta_{n+\vartheta}(\nabla \Delta u^\alpha)] \, \mathrm{d}v - \int_{\mathscr{S}} [\nabla w^\alpha \cdot (\nabla \delta u)] : [F^\beta_{n+\vartheta}(\nabla \Delta u^\alpha)] \, \mathrm{d}v$$

$$+ \vartheta \int_{\mathscr{S}} \nabla w^\alpha : \left[\frac{\mathrm{d}F^{\beta^\epsilon}}{\mathrm{d}\epsilon}(\nabla \Delta u^\alpha)^\epsilon \right]_{\epsilon=0} \mathrm{d}v + \int_{\mathscr{S}} \nabla w^\alpha : [F^\beta_{n+\vartheta}(\nabla \delta u^\alpha - \nabla u^\alpha \cdot \nabla \delta u)] \, \mathrm{d}v$$

$$+ \int_{\mathscr{S}} \nabla w^\alpha : [F^\beta_{n+\vartheta}(\nabla \Delta u^\alpha)][\mathbf{1} : \nabla \delta u] \, \mathrm{d}v = \Delta t \int_{\mathscr{S}} \nabla w^\alpha : [(\mathbf{1} - \nabla u^\beta)^{\mathrm{T}} \cdot \overline{D}^{\mathrm{p}} \cdot (\mathbf{1} - \nabla u^\beta)]_{n+\vartheta} \, \mathrm{d}v$$

$$- \Delta t \int_{\mathscr{S}} (\nabla w^\alpha \cdot \nabla \delta u) : [(\mathbf{1} - \nabla u^\beta)^{\mathrm{T}} \cdot \overline{D}^{\mathrm{p}} \cdot (\mathbf{1} - \nabla u^\beta)]_{n+\vartheta} \, \mathrm{d}v$$

$$+ \Delta t \vartheta \int_{\mathscr{S}} \nabla w^\alpha : \left[\frac{-\mathrm{d}(\nabla u^\beta)^{\mathrm{T}}}{\mathrm{d}\epsilon} \cdot \overline{D}^{\mathrm{p}} \cdot (\mathbf{1} - \nabla u^\beta) - (\mathbf{1} - \nabla u^\beta)^{\mathrm{T}} \cdot \overline{D}^{\mathrm{p}} \cdot \frac{\mathrm{d}(\nabla u^\beta)}{\mathrm{d}\epsilon} \right.$$

$$\left. + (\mathbf{1} - \nabla u^\beta)^{\mathrm{T}} \cdot \frac{\mathrm{d}\overline{D}^{\mathrm{p}}}{\mathrm{d}\epsilon} \cdot (\mathbf{1} - \nabla u^\beta) \right]_{\epsilon=0} \mathrm{d}v + \Delta t \int_{\mathscr{S}} \nabla w^\alpha : [(\mathbf{1} - \nabla u^\beta)^{\mathrm{T}} \cdot \overline{D}^{\mathrm{p}}$$

$$\cdot (\mathbf{1} - \nabla u^\beta)]_{n+\vartheta} [\mathbf{1} : (\nabla \delta u)] \, \mathrm{d}v. \tag{42}$$

Remark 1. Eq. (38) has the form where a specified functional of u^β must equal g. Such an integral form of the boundary condition is also seen in the Dirichlet-to-Neumann map, arising in the context of wave propagation in an infinite medium. In that case, the integral is over the boundary. In our case it is over the domain and involves ∇u^β and $\mathrm{curl}\, \varepsilon^{\beta^{-1}}$. The problem for u^β remains well-posed with such boundary conditions.

Remark 2. For a pure Neumann problem, $\partial\mathscr{B}_u = \emptyset$, and the effect of u^α on the β-scale weak form through the boundary term is lost. This is because no kinematic restrictions exist on the displacement, u, hence on u^β.

4. Finite element implementation

4.1. Bubnov–Galerkin approximations

The following Bubnov–Galerkin approximations of $(u^\alpha, u^\beta, \varepsilon^\beta)$ are made to solve equations (32), (33), and (28) respectively:

$$\boldsymbol{u}^{\beta^h} = \sum_{A=1}^{n_{np}} N_A \boldsymbol{d}_A^{\beta}, \quad \boldsymbol{w}^{\beta^h} = \sum_{A=1}^{n_{np}} N_A \boldsymbol{c}_A^{\beta}, \tag{43}$$

$$\boldsymbol{u}^{\alpha^h} = \sum_{A=1}^{n_{np}} N_A \boldsymbol{d}_A^{\alpha}, \quad \boldsymbol{w}^{\alpha^h} = \sum_{A=1}^{n_{np}} N_A \boldsymbol{c}_A^{\alpha}, \tag{44}$$

$$\boldsymbol{\varepsilon}^{\beta^h} = \sum_{A=1}^{n_{np}} N_A^{\mathscr{E}} \boldsymbol{d}_A^{\mathscr{E}}, \quad \boldsymbol{\Gamma}^{\beta^h} = \sum_{A=1}^{n_{np}} N_A^{\mathscr{E}} \boldsymbol{c}_A^{\mathscr{E}}. \tag{45}$$

The N_A are standard trilinear shape functions on hexahedral elements in three dimensions. The shape functions, $N_A^{\mathscr{E}}$, interpolating $\boldsymbol{\varepsilon}^{\beta^h}$, can be chosen to reintroduce incompatibility to the strain field by ensuring that $\mathrm{curl}\,\boldsymbol{\varepsilon}^{\beta^h} \neq \boldsymbol{0}$ in regions where strain gradient effects dominate. In practice, these interpolations should not be the gradients of any functions themselves. A sufficiently rich basis of functions can be used to ensure that the incompatibility is accurately reproduced. Suitable choices of such basis functions are currently being studied using different finite element spaces [13]. For the preliminary examples solved in Section 5 trilinear functions were used for $N_A^{\mathscr{E}}$. Thus interpolated, $\boldsymbol{\varepsilon}^{\beta^h}$ satisfies $\mathrm{curl}\,\boldsymbol{\varepsilon}^{\beta^h} \neq \boldsymbol{0}$.

4.2. Eq. solving—Newton–Raphson method

The equations are integrated in time by the Backward Euler algorithm, linearized (see Appendices A.1 and A.2), and the following system of matrix equations is obtained for β- and α-scales respectively.

$$\boldsymbol{K}_1^{\alpha}\delta\boldsymbol{d}^{\alpha} + \boldsymbol{K}_1^{\beta}\delta\boldsymbol{d}^{\beta} = \boldsymbol{R}_1, \tag{46}$$

$$\boldsymbol{K}_2^{\alpha}\delta\boldsymbol{d}^{\alpha} + \boldsymbol{K}_2^{\beta}\delta\boldsymbol{d}^{\beta} = \boldsymbol{R}_2. \tag{47}$$

Note that $\boldsymbol{R}_1 := \boldsymbol{F}^{\mathrm{ext}} - \boldsymbol{F}^{\mathrm{int}}$ represents the difference of external and internal forces and that the unknowns in these equations are solved for using a staggered Newton–Raphson algorithm (Box 1). The matrix form of Eq. (28) is:

$$\boldsymbol{M}\boldsymbol{d}^{\mathscr{E}} = \boldsymbol{G}\boldsymbol{d}^{\beta}. \tag{48}$$

5. Numerical results

Two numerical examples are considered in this section. The first demonstrates the local evolution of the model under nonuniform loading. The second is a comparison against experiments on the torsion of thin wires. This example is a check on both: the theoretical formulation and its numerical implementation.

5.1. Local evolution of the model

A cubic micron of Tantalum was loaded by prescribing displacements that vary linearly along the $X1$-axis (see Fig. 5) to induce strain gradients. Box 2 shows material parameters and model data. The loading causes linear gradients in several of the strain components and demonstrates the influence of strain gradients upon different stress components. The tensor $\overline{\boldsymbol{\zeta}}$ has the effect of a back stress upon final results and will be referred to as such for the remainder of this section.

```
n = 0
time step loop
   k = 0
```
$$\boldsymbol{d}^{\beta^{(i,k)}} = \boldsymbol{d}_n^\beta \qquad\qquad \boldsymbol{d}^{\alpha^{(j,k)}} = \boldsymbol{d}_n^\alpha$$
```
   stagger iteration loop
       β-scale equation:  (i=0) start iteration loop
           if    (‖R̂₁^(0,k)‖ < ε₁‖R̂₁^(0,0)‖   or   ‖R̂₁^(0,k)‖ < ε₂)  then
```
$$\boldsymbol{d}_{n+1}^\alpha = \boldsymbol{d}^{\alpha^{(j+1,k)}} \qquad\qquad \boldsymbol{d}_{n+1}^\beta = \boldsymbol{d}^{\beta^{(i+1,k)}}$$
```
               n ← n+1   (converges with α-scale solve solution:  next step)
           else
```
$$\boldsymbol{K}_1^\beta(\boldsymbol{d}^{\alpha^{(j,k)}}, \boldsymbol{d}^{\beta^{(i,k)}})\delta\boldsymbol{d}^{\beta^{(i,k)}} = \hat{\boldsymbol{R}}_1^{(i,k)}$$
$$:= \boldsymbol{F}_{1(n+1)}^{\text{ext}} - (\boldsymbol{F}_{1(n+1)}^{\text{int}}(\boldsymbol{d}^{\alpha^{(j,k)}}, \boldsymbol{d}^{\beta^{(i,k)}}) + \boldsymbol{K}_1^\alpha \delta\boldsymbol{d}^{\alpha^{(j,k)}})$$
$$\boldsymbol{d}^{\beta^{(i+1,k)}} = \boldsymbol{d}^{\beta^{(i,k)}} + \delta\boldsymbol{d}^{\beta^{(i,k)}}$$
```
               if    (‖R̂₁^(i,k)‖ < ε₁‖R̂₁^(0,0)‖   or    ‖R̂₁^(i,k)‖ < ε₂   or   i > i^max)      then
                   exit β-scale equation iteration loop
               else
                   continue β-scale equation iteration loop
               endif
           endif
       end loop (β-scale equation solver)
       Solve dᴱ = M⁻¹Gd^(β(i+1,k))
       α-scale equation:  (j=0) start iteration loop
           if    (‖R̂₂^(0,k)‖ < ε₁‖R̂₂^(0,0)‖   or   ‖R̂₂^(0,k)‖ < ε₂)  then
```
$$\boldsymbol{d}_{n+1}^\alpha = \boldsymbol{d}^{\alpha^{(j+1,k)}} \qquad\quad \boldsymbol{d}_{n+1}^\beta = \boldsymbol{d}^{\beta^{(i+1,k)}} \qquad\quad \boldsymbol{d}_{n+1}^\mathcal{E} = \boldsymbol{d}^\mathcal{E}$$
```
               n ← n+1   (converges with β-scale solve solution:  next step)
           else
```
$$\boldsymbol{K}_2^\alpha(\boldsymbol{d}^{\alpha^{(j,k)}}, \boldsymbol{d}^{\beta^{(i,k)}})\delta\boldsymbol{d}^{\alpha^{(j,k)}} = \hat{\boldsymbol{R}}_2^{(j,k)}$$
$$:= \boldsymbol{R}_2 - \boldsymbol{K}_2^\beta \delta\boldsymbol{d}^{\beta^{(i,k)}}$$
$$\boldsymbol{d}^{\alpha^{(j+1,k)}} = \boldsymbol{d}^{\alpha^{(j,k)}} + \delta\boldsymbol{d}^{\alpha^{(j,k)}}$$
```
               if    (‖R̂₂^(j,k)‖ < ε₁‖R̂₂^(0,0)‖   or    ‖R̂₂^(j,k)‖ < ε₂   or   j > j^max) then
                   exit α-scale equation iteration loop
               else
                   continue α-scale equation iteration loop
               endif
           endif
       end loop (α-scale equation solver)
     if  (k < k^max) then:
         k ← k+1
     else
         exit algorithm (no convergence after k^max iterations)
     endif
   end loop (equation staggering)
end loop (time step)
```

Box 2 (Material parameters for nonuniformly-loaded cube).

Young's modulus E: 168 GPa   Poisson's ratio v: 0.34
Length scale l (see Eq. (5)):   1e−6 m
Gradient parameter c_ζ (see Eq. (9)):   4.9
Prescribed displacements: 0.12 μm (End)   0.06 μm (Center)   (constant in X3)
Supports: All fixed (constant in X3)

The tensors $\overline{\alpha}_l^e$ and $\overline{\zeta}$ resulting from the curl($\bullet$) operation possess the following characteristics: Stresses and strains with dominant normal directions may produce back stress terms with dominant shear directions and vice-versa. For the case at hand, for example, the Cauchy stress component σ_{22} and displacement gradient $u_{2,2}^\beta$ dominate. However, their gradients—which are also dominant—will appear in off diagonal curl(ε^β) and back stress $\overline{\zeta}$ components, and therefore affect off-diagonal stress components (Fig. 6). As a consequence, though σ_{22} is dominant, it is not necessarily affected by the back stress. This is apparent when
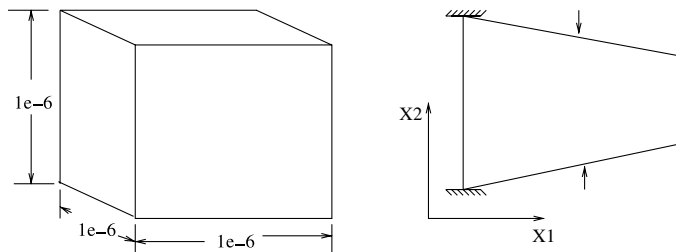
Fig. 5. Micron sized cube specimen: one square micron of tantalum in compression (left) and prescribed displacements along $X1$ in $X2$ induce a strain gradient (right).
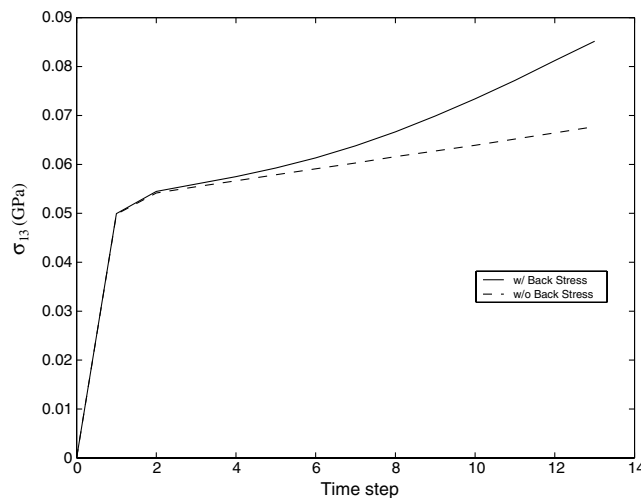
Fig. 6. Back-stress providing a hardening effect on σ_{13}.
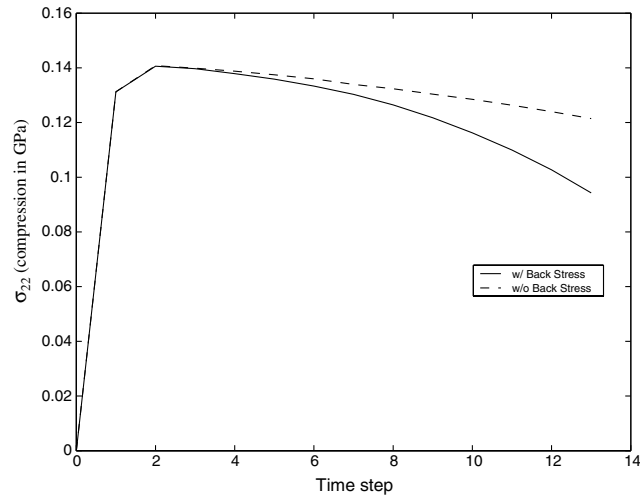
Fig. 7. Back-stress providing a softening effect on σ_{22} at a point near the support.
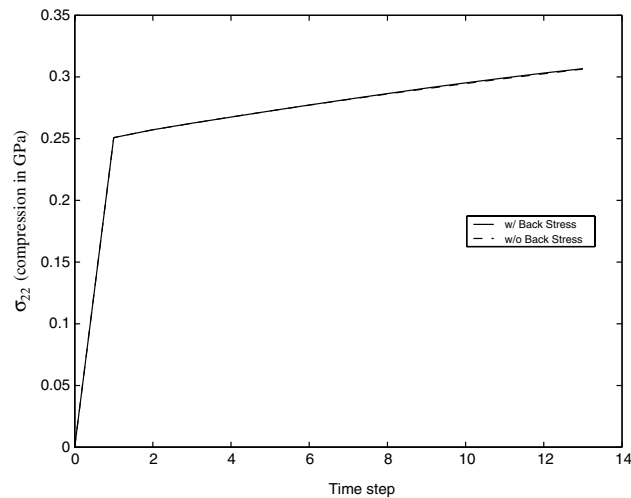
Fig. 8. Back-stress having negligible effect on σ_{22} at point near center of cube.

Fig. 7 is compared to Fig. 8. In Fig. 7, stress is sampled close to the support where shear is prevalent, how-ever, in Fig. 8, stress is sampled at a point where shear stresses are smaller. These characteristics also are inherited by the back stress tensor $\bar{\zeta}$.

Fig. 9 shows fields for various components of $\bar{\zeta}$. Recall that this tensor represents the influence of incom-patibilities as a back stress. An interesting observation is that these fields are more circular in appearance. Small point-like areas of high back stress values appear as seen in Fig. 9(a,c).

As shown by this simple example, the applied strain gradients induce back stress, and therefore harden-ing, in what one may describe as a noncoaxial manner for the chosen theoretical formulation.
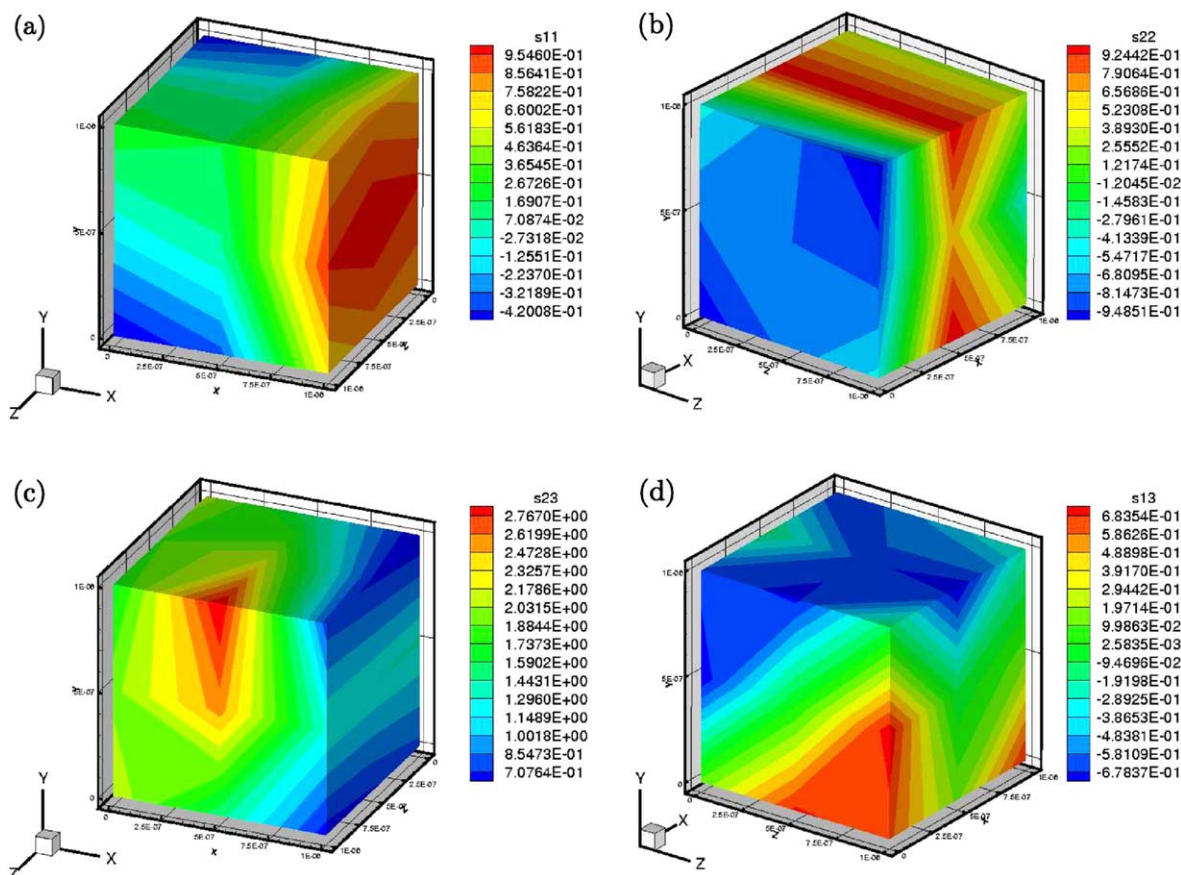
Fig. 9. Back stress fields as a result of strain gradient curlε^β: (a) $\zeta_{1.1}^{(sym)}$ (GPa), (b) $\zeta_{2.2}^{(sym)}$ (GPa), (c) $\zeta_{2.3}^{(sym)}$ (GPa) and (d) $\zeta_{1.3}^{(sym)}$ (GPa).

5.2. Comparison with microtorsion experiments

The numerical simulations described in this section were motivated by the microtorsion experiments seen in the work of Fleck and co-workers [14]. In that paper, the authors observed size effects playing important roles in the response of polycrystalline materials subjected to various loadings, particularly for micron scale specimens. Specifically, the observation was that the smaller the size, the harder the plastic response. The authors went on to postulate that yield stress depends upon strain gradients as well as strain.

Fleck and co-workers measured the torsional responses of copper wires in order to obtain direct experimental evidence for strain gradient hardening. The wires were made of polycrystalline copper and varied in diameter from 12 to 170 μm. It was predicted that the thinner wires would have greater strain gradients (and a corresponding greater amount of geometrically necessary dislocations), and would consequently experience a greater degree work hardening. The experimental results discussed in that paper confirm this expectation and the thinner work hardened wires were indeed stronger than the thicker ones. To establish measures of torque, Q, and twist per unit length, κ, that were independent of wire radius, a, dimensional groups Q/a^3 and κa were used. With these groups, Q/a^3 is a function of κa but is otherwise independent of radius a.

The simulation discussed below is a preliminary one. Simplicity was a consideration and an exact replication of the experimental results seen in [14] was not expected. More accurate microtorsion simulations
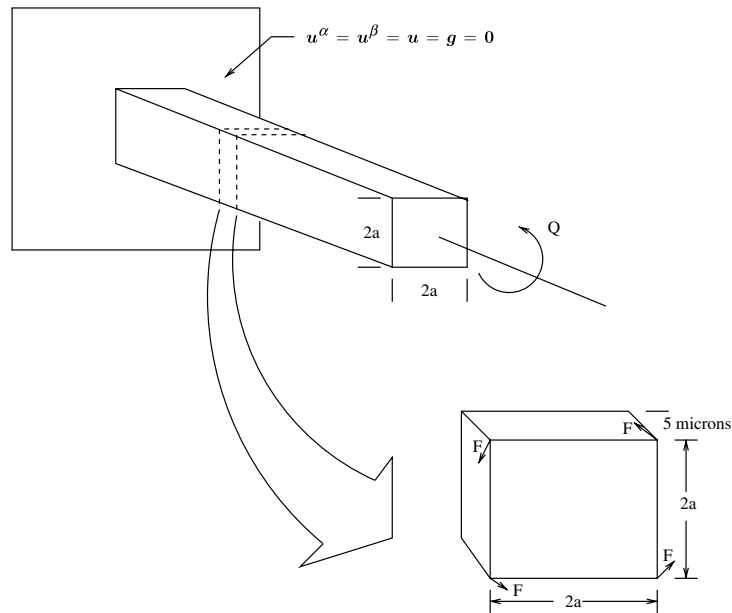
Fig. 10. A rectangular member subjected to torsion.

are left for future work. A long thin member of square cross section was selected as a torsion specimen (see Fig. 10). Because the angles of twist per unit length applied to the wire in the [14] experiment were very large (on the order of 0.1 rad/μm), a small cross sectional slice of the member seen in Fig. 10 was used for the numerical simulation, this way smaller rotations could be used for easier boundary condition implementation. This small slice is depicted in Fig. 10. The applied torque is administered to the slice by applying forces at its four corners (denoted by F in the figure). The FEA mesh of the slice is shown in Fig. 11. The dimensions of this geometry are $2a \times 2a \times 5$ μm, where the dimension $2a$ is analogous to the diameter of the copper wire cited above. Box 3 below shows material parameters and model data.

Box 3 (Material parameters for microtorsion simulations).

Young's modulus E: 124 GPa   Poisson's ratio v: 0.34
Length scale l (see Eq. (5)): 1e−6 m
Gradient parameter c_ζ (see Eq. (9)): 1.01
BCJ parameters: $V = 14.0$ $f = 15.8$ $Y = 0.63$
Applied moment at final time was $\frac{Q}{a^3} = 300$ MPa

For a fixed set of material parameters (Box 3), the normalized torques were plotted against twist for three wire diameters (Fig. 12). Observe the increase in normalized torque with decrease in wire width. While the comparison with experiment is far from perfect, the simulation results have the expected trend. This set of results demonstrates the length scale effect of the strain gradient plasticity model, and its reproduction when the model is implemented with the variational multiscale method.
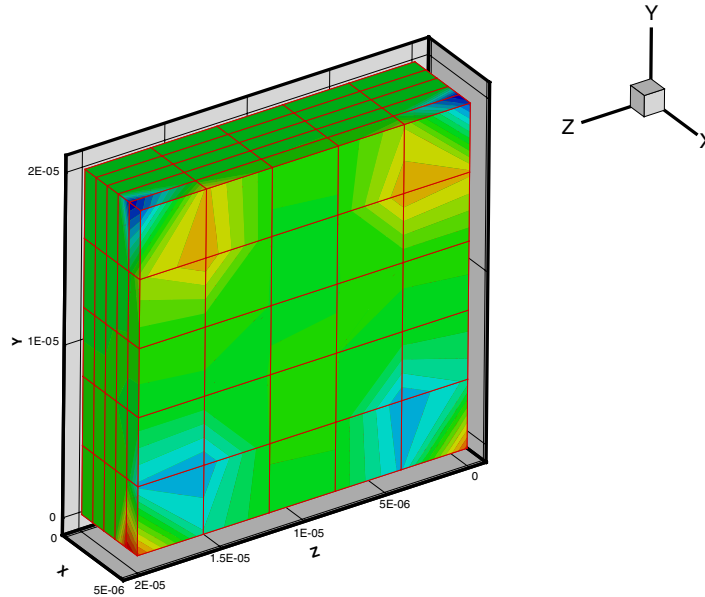
Fig. 11. Finite element mesh of the cross-sectional slice seen in Fig. 10. Contours in this figure are of $\overline{\zeta}_{13}$.
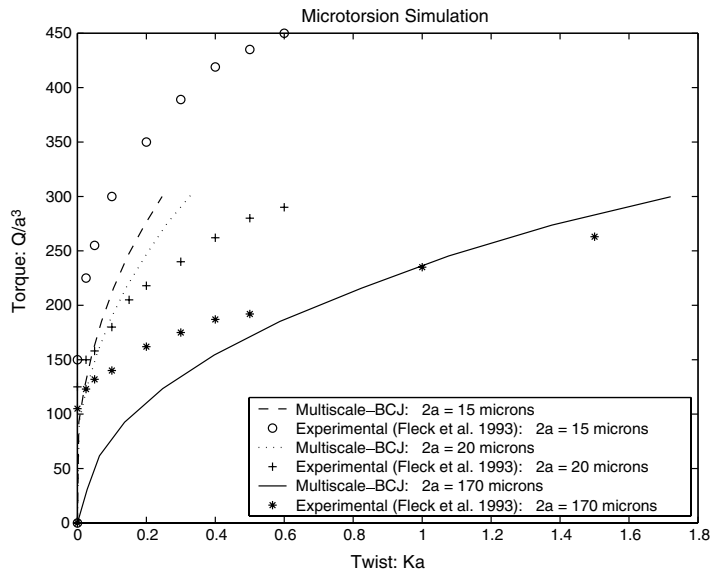
Fig. 12. The response of three micron scale wires of differing diameters subjected to torsion. Plotted above is both the simulated response and experimental data.

6. Conclusions

The ideas presented in this paper are part of a body of work in which variational methods have been developed for embedding several models of fine scale physics in the macromechanical formulation of solid

mechanics. In previous work [17,18] the fine scale physics has consisted of surface laws and a complete theory for strain gradient plasticity. In a departure, this paper views a particular phenomenological plasticity model as the fine scale (here, called the α-scale) model. This view is justified since the flow rule of the phenomenological plasticity model incorporates the gradient of plastic strain to model many phenomena observed at fine scales (see Section 1). Of greater importance is the fact that the inclusion of the plastic strain gradient leads to several mathematical and computational difficulties. These include the integration of the plasticity model, which is now described by a partial differential equation, and the specification of boundary conditions on the plastic strain. Some of these are mitigated by the multiscale approach adopted here.

The specific multiscale decomposition used here, by which the α-scale strain is identified with the plastic deformation gradient leads to its own difficulty in the vanishing of the Nye dislocation density tensor. A strain field, ε^β, has been introduced and weakly related to the gradient of the β-scale displacement to circumvent this difficulty (Section 3.1.2). However, the fidelity of the resulting numerical representation of incompatibilities depends much too strongly on the interpolation functions for ε^β. It also amounts to an expansion in the number of unknown fields. The underlying assumption of a multiscale decomposition of the displacement clearly needs refinement for this problem. One alternative is to introduce a multiscale decomposition directly on the strain field. We will return to this topic in future work.

The results presented here are preliminary ones. They are meant to only demonstrate the working of the computational formulation and some features of the assumed plasticity model. Work is in progress on improved theoretical models of gradient theories incorporating incompatibilities (dislocations and disclinations), and on the use of fundamentally different classes of finite element spaces to represent the Nye dislocation density tensor.

Acknowledgments

Appendix A. Linearization

A.1. α-scale equation

Recall the α-scale equation in its weak form from Eq. (31).

$$(\mathscr{W}^\alpha)\int_{\mathscr{S}} \nabla w^\alpha : \left[F^\beta \cdot \nabla \dot{u}^\alpha\right] \mathrm{d}v = \int_{\mathscr{S}} \nabla w^\alpha : \left[(1 - \nabla u^\beta)^{\mathrm{T}} \cdot \overline{D}^{\mathrm{p}} \cdot (1 - \nabla u^\beta)\right] \mathrm{d}v. \tag{A.1}$$

Expanding the ∇ operator, and substituting Eq. (27) into Eq. (A.1).

$$\int_{\mathscr{S}} \nabla w^\alpha : \left[F^\beta \left(\frac{\partial \dot{u}^\alpha}{\partial X} F^{-1}\right)\right] \mathrm{d}v = \int_{\mathscr{S}} \nabla w^\alpha : \left[F^{\beta-\mathrm{T}} \overline{D}^\alpha F^{\beta-1}\right] \mathrm{d}v. \tag{A.2}$$

Recognizing $\frac{\partial \dot{u}^\alpha}{\partial X} = \dot{F}^\alpha$, Eq. (A.2) can be written:

$$\int_{\mathscr{S}} \nabla \boldsymbol{w}^{\alpha} : \left[\boldsymbol{F}^{\beta} \dot{\boldsymbol{F}}^{\alpha} \boldsymbol{F}^{-1} \right] \mathrm{d}v = \int_{\mathscr{S}} \nabla \boldsymbol{w}^{\alpha} : \left[\boldsymbol{F}^{\beta^{-\mathrm{T}}} \overline{\boldsymbol{D}}^{\alpha} \boldsymbol{F}^{\beta^{-1}} \right] \mathrm{d}v. \tag{A.3}$$

From Eq. (13), the plastic flow equation is written in terms of the α-scale field:

$$\overline{\boldsymbol{D}}^{\alpha} = \underbrace{\sqrt{\frac{3}{2}} f \left\langle \sinh \left[\frac{\overline{\Xi}^{\mathrm{eff}} - (\kappa b + Y)}{V} \right]^{=:\beta} \right\rangle}_{=:\phi} \overline{\boldsymbol{N}}^{\alpha}, \tag{A.4}$$

$$\overline{\boldsymbol{D}}^{\alpha} = \phi \overline{\boldsymbol{N}}^{\alpha}. \tag{A.5}$$

Substituting (A.5) into Eq. (A.3) and using the Backward Euler Algorithm, Eq. (A.3) in time-discretized form is:

$$\int_{\mathscr{S}} \nabla \boldsymbol{w}^{\alpha} : \left[\boldsymbol{F}^{\beta} \left(\frac{\boldsymbol{F}^{\alpha} - \boldsymbol{F}^{\alpha}_{n}}{\Delta t} \right) \boldsymbol{F}^{-1} \right] \mathrm{d}v = \int_{\mathscr{S}} \nabla \boldsymbol{w}^{\alpha} : \left[\phi \boldsymbol{F}^{\beta^{-\mathrm{T}}} \overline{\boldsymbol{N}}^{\alpha} \boldsymbol{F}^{\beta^{-1}} \right] \mathrm{d}v. \tag{A.6}$$

Combining integrals and expanding terms of Eq. (A.6), we define:

$$\mathscr{G}_2 := \int_{\mathscr{S}} \nabla \boldsymbol{w}^{\alpha} : \left[\boldsymbol{1} - \boldsymbol{F}^{\beta} \boldsymbol{F}^{\alpha}_{n} \boldsymbol{F}^{-1} - \Delta t \phi \boldsymbol{F}^{\beta^{-\mathrm{T}}} \overline{\boldsymbol{N}}^{\alpha} \boldsymbol{F}^{\beta^{-1}} \right] \mathrm{d}v = 0. \tag{A.7}$$

For variations $\delta \boldsymbol{u}^{\alpha}$ and $\delta \boldsymbol{u}^{\beta}$, the variation in $\mathscr{G}_2$ is:

$$\delta \mathscr{G}_2 = \int_{\mathscr{S}} \nabla \boldsymbol{w}^{\alpha} : \left[\delta \left(-\boldsymbol{F}^{\beta} \boldsymbol{F}^{\alpha}_{n} \boldsymbol{F}^{-1} \right) - \Delta t \delta \left(\phi \underbrace{\boldsymbol{F}^{\beta^{-\mathrm{T}}} \overline{\boldsymbol{N}}^{\alpha} \boldsymbol{F}^{\beta^{-1}}}_{=:N} \right) \right] \mathrm{d}v = 0. \tag{A.8}$$

Linearizing terms, Eq. (A.8) is written:

$$\delta \mathscr{G}_2 = \int_{\mathscr{S}} \nabla \boldsymbol{w}^{\alpha} : \left[-\delta \boldsymbol{F}^{\beta} \boldsymbol{F}^{\alpha}_{n} \boldsymbol{F}^{-1} - \boldsymbol{F}^{\beta} \boldsymbol{F}^{\alpha}_{n} \delta \boldsymbol{F}^{-1} - \Delta t \delta \phi N - \Delta t \phi \delta N \right] \mathrm{d}v = 0. \tag{A.9}$$

Details are provided in [12].

A.2. β-scale equation

For variations $\delta \boldsymbol{u}^{\alpha}$ and $\delta \boldsymbol{u}^{\beta}$, the variation in Eq. (33) is defined:

$$\delta \mathscr{G}_1 := \delta \left(\int_{\mathscr{S}} \nabla \boldsymbol{w}^{\beta} : \boldsymbol{\sigma} - \int_{\partial \mathscr{B}_t} \boldsymbol{w}^{\beta} \cdot \boldsymbol{t} \mathrm{d}a - \int_{\mathscr{S}} \boldsymbol{w}^{\beta} \cdot \boldsymbol{b} \mathrm{d}v \right) \neq 0.$$

Working with the first term:

$$\delta \left(\int_{\mathscr{S}_{\mathrm{t}}} \nabla \boldsymbol{w}^{\beta} : \boldsymbol{\sigma} \mathrm{d}v \right) = \int_{\mathscr{B}} \delta \left[\left(\frac{\partial \boldsymbol{w}^{\beta}}{\partial \boldsymbol{X}} \boldsymbol{F}^{-1} \right) : \boldsymbol{\tau} \right] \mathrm{d}V$$

$$= \underbrace{- \int_{\mathscr{B}} \nabla \boldsymbol{w}^{\beta} : \boldsymbol{\tau} (\nabla \delta \boldsymbol{u}^{\alpha})^{\mathrm{T}} \mathrm{d}V}_{I^{\alpha}}$$

$$\times \underbrace{- \int_{\mathscr{B}} \nabla \boldsymbol{w}^{\beta} : \boldsymbol{\tau} (\nabla \delta \boldsymbol{u}^{\beta})^{\mathrm{T}} \mathrm{d}V}_{I^{\beta}} + \underbrace{\int_{\mathscr{B}} \nabla \boldsymbol{w}^{\beta} : \delta \boldsymbol{\tau} \mathrm{d}V}_{\mathrm{II}}. \tag{A.10}$$

Working with term II:

$$\text{II} = \underbrace{\int_{\mathscr{B}} \nabla \boldsymbol{w}^\beta : [\delta(\boldsymbol{F}^\beta)\overline{\mathbf{S}}\boldsymbol{F}^{\beta\mathrm{T}} + \boldsymbol{F}^\beta\overline{\mathbf{S}}\delta(\boldsymbol{F}^{\beta\mathrm{T}})]\,\mathrm{d}V}_{\text{IIA}} + \underbrace{\int_{\mathscr{B}} \nabla \boldsymbol{w}^\beta : \boldsymbol{F}^\beta\delta(\overline{\mathbf{S}})\boldsymbol{F}^{\beta\mathrm{T}}\,\mathrm{d}V}_{\text{IIB}}.$$

Rewriting the integral in the current configuration, the sum of terms I^α, I^β, and IIA is:

$$-\int_{\mathscr{S}} \nabla \boldsymbol{w}^\beta : (\boldsymbol{\sigma}(\nabla \delta \boldsymbol{u}^\alpha)^\mathrm{T}\boldsymbol{F}^{\beta\mathrm{T}})\,\mathrm{d}v + \int_{\mathscr{S}} \nabla \boldsymbol{w}^\beta : (\nabla \delta \boldsymbol{u}^\beta \boldsymbol{\sigma})\,\mathrm{d}v - \int_{\mathscr{S}} \nabla \boldsymbol{w}^\beta : (\boldsymbol{F}^\sharp \nabla \delta \boldsymbol{u}^\alpha \boldsymbol{\sigma})\,\mathrm{d}v.$$

Noting that: $\mathbb{C} : \delta\mathbf{E}^\beta = \mathbb{C} : (\boldsymbol{F}^{\beta\mathrm{T}}\delta\boldsymbol{F}^\beta)$ where: $\delta\boldsymbol{F}^\beta = [\nabla\delta\boldsymbol{u}^\beta - \boldsymbol{F}^\sharp\nabla\delta\boldsymbol{u}^\alpha]\boldsymbol{F}^\beta$,

$$\text{IIB} = \int_{\mathscr{B}} \nabla \boldsymbol{w}^\beta : \boldsymbol{F}^\beta[\mathbb{C} : (\boldsymbol{F}^{\beta\mathrm{T}}[\nabla\delta\boldsymbol{u}^\beta - \boldsymbol{F}^\sharp\nabla\delta\boldsymbol{u}^\alpha]\boldsymbol{F}^\beta)]\boldsymbol{F}^{\beta\mathrm{T}}\,\mathrm{d}V = \int_{\mathscr{B}} \nabla \boldsymbol{w}^\beta : \boldsymbol{F}^\beta[\mathbb{C}$$

$$: (\boldsymbol{F}^{\beta\mathrm{T}}\nabla\delta\boldsymbol{u}^\beta\boldsymbol{F}^\beta)]\boldsymbol{F}^{\beta\mathrm{T}}\,\mathrm{d}V - \int_{\mathscr{B}} \nabla \boldsymbol{w}^\beta : \boldsymbol{F}^\beta[\mathbb{C} : (\boldsymbol{F}^{\beta\mathrm{T}}\boldsymbol{F}^\sharp\nabla\delta\boldsymbol{u}^\alpha\boldsymbol{F}^\beta)]\boldsymbol{F}^{\beta\mathrm{T}}\,\mathrm{d}V.$$

Switching to indicial notation.

$$= \int_{\mathscr{B}} w_{i,j}^\beta F_{iI}^\beta[\mathbb{C}_{IJKL}F_{Kk}^{\beta\mathrm{T}}\delta u_{k,l}^\beta F_{l,L}^\beta]F_{J,j}^{\beta\mathrm{T}}\,\mathrm{d}V - \int_{\mathscr{B}} w_{i,j}^\beta F_{iI}^\beta[\mathbb{C}_{IJKL}F_{Kk}^{\beta\mathrm{T}}F_{ks}^\sharp\delta u_{s,l}^\beta F_{l,L}^\beta]F_{J,j}^{\beta\mathrm{T}}\,\mathrm{d}V.$$

Rearranging and writing the integral in the current configuration.

$$= \int_{\mathscr{S}} w_{i,j}^\beta \underbrace{\frac{1}{j}F_{iI}^\beta F_{jJ}^\beta F_{kK}^\beta F_{lL}^\beta\mathbb{C}_{IJKL}}_{=:\mathbf{c}^\beta}\,\delta u_{k,l}^\beta\,\mathrm{d}v - \int_{\mathscr{S}} w_{i,j}^\beta \underbrace{\frac{1}{j}F_{iI}^\beta F_{jJ}^\beta F_{kK}^\beta F_{lL}^\beta\mathbb{C}_{IJKL}}_{=\mathbf{c}^\beta}\,F_{ks}^\sharp\delta u_{s,l}^\beta\,\mathrm{d}v. \qquad (\text{A.11})$$

Defining:

$$\mathscr{S}(\delta\boldsymbol{u}^\alpha, \delta\boldsymbol{u}^\beta) := -\boldsymbol{\sigma}(\nabla\delta\boldsymbol{u}^\alpha)^\mathrm{T}\boldsymbol{F}^{\beta\mathrm{T}} + \nabla\delta\boldsymbol{u}^\beta\boldsymbol{\sigma} - \boldsymbol{F}^\sharp\nabla\delta\boldsymbol{u}^\alpha\boldsymbol{\sigma} + \mathbf{c}^\beta : \nabla\delta\boldsymbol{u}^\beta - \mathbf{c}^\beta : \boldsymbol{F}^\sharp\nabla\delta\boldsymbol{u}^\alpha,$$

where $\mathbf{c}_{ijkl}^\beta := \frac{1}{j}F_{iI}^\beta F_{jJ}^\beta F_{kK}^\beta F_{lL}^\beta\mathbb{C}_{IJKL}$ and $\boldsymbol{F}^\sharp := \nabla\boldsymbol{u}^\beta\boldsymbol{F}^\beta$

we can compactly express:

$$\delta\mathscr{G}_1 = \int_{\mathscr{S}} \nabla\boldsymbol{w}^\beta : \mathscr{S}(\delta\boldsymbol{u}^\alpha, \delta\boldsymbol{u}^\beta)\,\mathrm{d}v + \int_{\partial\mathscr{B}_t} \boldsymbol{w}^\beta \cdot [\mathscr{S}(\delta\boldsymbol{u}^\alpha, \delta\boldsymbol{u}^\beta) \cdot n]\,\mathrm{d}a.$$

From this linearization, the expression $\mathscr{G}_2 + \delta\mathscr{G}_2 = 0$ leads to Eq. (46).

References

[1] A. Acharya, J.L. Bassani, A. Beaudoin, Geometrically necessary dislocations, hardening, and a simple gradient theory of crystal plasticity, Scr. Mater. 48 (2003) 167–172.

[2] F. Armero, K. Garikipati, An analysis of strong discontinuities in multiplicative finite strain plasticity and their relation with the numerical simulation of strain localization in solids, Int. J. Solids Struct. 33 (1996) 2863–2885.

[3] A. Arsenlis, D.M. Parks, Crystallographic aspects of geometrically-necessary and statistically-stored dislocation density, Acta Mater. 47 (5) (1999) 1597–1611.

[4] M.F. Ashby, The deformation of plastically non-homogeneous materials, Philos. Mag. 21 (1970) 339–424.

[5] D.J. Bammann, Modeling the temperature and strain rate dependent large deformation of metals, Appl. Mech. Rev. 43 (1990) S312–S319.

[6] D.J. Bammann, A model of crystal plasticity containing a natural length scale, Mater. Sci. Engrg. A 309–310 (2001) 406–410.

[7] B.A. Bilby, R. Bullough, E. Smith, Continuous distributions of dislocations: a new application of the methods of non-Riemannian geometry, Proc. Roy. Soc. Lond. Ser. A 231 (1955) 263–273.

[8] E. Bittencourt, A. Needleman, M.E. Gurtin, E. Van der Giessen, A comparison of nonlocal continuum and discrete dislocation plasticity predictions, J. Mech. Phys. Solids 51 (2003) 281–310.
 [9] P. Cermelli, M.E. Gurtin, On the characterization of geometrically necessary dislocations in finite plasticity, J. Mech. Phys. Solids 49 (2001) 1539–1568.
[10] B.D. Coleman, M.E. Gurtin, Thermodynamics with internal state variables, J. Chem. Phys. 47 (1967) 597–613.
[11] B.D. Coleman, W. Noll, The thermodynamics of elastic materials with heat conduction and viscosity, Arch. Ration. Mech. Anal. 13 (1963) 167–178.
[12] S.L. Creighton, Embedding models of fine scale physics in the macromechanical continuum formulation of solid mechanics by variational multiscale techniques, Ph.D. thesis, University of Michigan, 2003.
[13] P.A. Dixit, R.A. Regueiro, K. Garikipati, Numerical formulation of an incompatibility-based strain gradient plasticity model using vector finite element spaces, in preparation.
[14] N.A. Fleck, G.M. Muller, M.F. Ashby, J.W. Hutchinson, Strain gradient plasticity: theory and experiment, Acta Metall. Mater. 42 (1994) 475–487.
[15] N.A. Fleck, M.F. Ashby, J.W. Hutchinson, The role of geometrically necessary dislocations in giving material strengthening, Scr. Mater. 48 (2003) 179–183.
[16] H. Gao, Y. Huang, Geometrically necessary dislocation and size-dependent plasticity, Scr. Mater. 48 (2003) 113–118.
[17] K. Garikipati, A variational multiscale method to embed micromechanical surface laws in the macromechanical continuum formulation, Comput. Model. Engrg. Sci. 3 (2) (2002) 175–184.
[18] K. Garikipati, Variational multiscale methods to embed the macromechanical continuum formulation with fine scale strain gradient theories, Int. J. Numer. Methods Engrg. 57 (9) (2003) 1283–1298.
[19] K. Garikipati, T.J.R. Hughes, A variational multiscale approach to strain localization—formulation for multidimensional problems, Comput. Methods Appl. Mech. Engrg. 188 (2000) 39–60.
[20] F. Garofalo, C. Richmond, W.F. Domis, F. von Gemmingen, Strain–time, rate–stress and rate–temperature relations during large deformations in creep, in: Joint International Conference on Creep, vol. 1, 1963, pp. 31–39.
[21] M.E. Gurtin, A gradient theory of single-crystal viscoplasticity that accounts for geometrically necessary dislocations, J. Mech. Phys. Solids 50 (2002) 5–32.
[22] D.A. Hughes, Q. Liu, D.C. Chrzan, N. Hansen, Scaling of microstructural parameters: misorientations of deformation induced boundaries, Acta Mater. 45 (1997) 105–112.
[23] D.A. Hughes, N. Hansen, D.J. Bammann, Geometrically necessary boundaries, incidental dislocation boundaries and geometrically necessary dislocations, Scr. Mater. 48 (2003) 147–153.
[24] D. Klahn, A.V. Mukherjee, J.E. Dorn, Strain-rate effects, in: Second International Conference on the Strength of Metals and Alloys, American Society for Metals, Metals Park, OH, 1970, pp. 951–982.
[25] K. Kondo, On the geometrical and physical foundations of the theory of yielding, in: Proceedings of the 2nd Japan National Congress for Appl. Mech., 1952, pp. 41–47.
[26] E. Kröner, Allgemeine kontinuumstheorie der versetzungen und eigenspannungen, Arch. Ration. Mech. Anal. 4 (1960) 273–334.
[27] E. Kröner, Benefits and shortcomings of the continuous theory of dislocations, Int. J. Solids Struct. 38 (2001) 1115–1134.
[28] L.P. Kubin, A. Mortensen, Geometrically necessary dislocations and strain-gradient plasticity: a few critical issues, Scr. Mater. 48 (2003) 119–125.
[29] E.H. Lee, Elastic–plastic deformation at finite strains, ASME J. Appl. Mech. 36 (1969) 1–6.
[30] E.H. Lee, D.T. Liu, Finite-strain elastic–plastic theory with application to plane-wave analysis, J. Appl. Phys. 38 (1967) 19–27.
[31] J. Mandel, Thermodynamics and plasticity, in: J.J. Delgado, et al. (Eds.), Foundations of Continuum Thermodynamics, Macmillan, New York, 1974, pp. 283–304.
[32] P.M. Naghdi, A.R. Srinivasa, A dynamical theory of structured solids. I. Basic developments, Phil. Trans. Roy. Soc. Lond. Ser. A 345 (1993) 425–458.
[33] A. Needleman, J.Gil Sevillano, Preface to the viewpoint set on: geometrically necessary dislocations and size dependent plasticity, Scr. Mater. 48 (2003) 109–111.
[34] J.F. Nye, Some geometrical relations in dislocated crystals, Acta Metall. 1 (1953) 153–162.
[35] R.A. Regueiro, D.J. Bammann, E.B. Marin, K. Garikipati, A nonlocal phenomenological anisotropic finite deformation plasticity model accounting for dislocation defects, ASME J. Engrg. Mat. Tech. 124 (2002) 380–387.
[36] P. Steinmann, Views on multiplicative elastoplasticity and the continuum theory of dislocations, Int. J. Engrg. Sci. 34 (1996) 1717–1735.
[37] E.B. Tadmor, R. Phillips, M. Ortiz, Hierarchical modeling in the mechanics of materials, Int. J. Solids Struct. 37 (2000) 379–389.
[38] C. Teodosiu, F. Sidoroff, A finite theory of the elastovisoplasticity of single crystals, Int. J. Engrg. Sci. 14 (1976) 713–723.
[39] M. Zaiser, E.C. Aifantis, Geometrically necessary dislocations and strain gradient plasticity—a dislocation dynamics point of view, Scr. Mater. 48 (2003) 133–139.
[40] H.M. Zbib, E.C. Aifantis, Size effects and length scales in gradient plasticity and dislocation dynamics, Scr. Mater. 48 (2003) 155–160.